

## Temporal variability of nitrogen fixation and particulate nitrogen export at Station ALOHA

Daniela Böttjer,<sup>1,2</sup> John E. Dore,<sup>3</sup> David M. Karl,<sup>1,2</sup> Ricardo M. Letelier,<sup>2,4</sup> Claire Mahaffey,<sup>5</sup> Samuel T. Wilson,<sup>1,2</sup> Jonathan Zehr,<sup>2,6</sup> Matthew J. Church\*<sup>1,2</sup>

<sup>1</sup>Department of Oceanography, School of Ocean and Earth Science and Technology, University of Hawai'i at Mānoa, Honolulu, Hawai'i

<sup>2</sup>Daniel K. Inouye Center for Microbial Oceanography: Research and Education, University of Hawai'i at Mānoa, Honolulu, Hawai'i

<sup>3</sup>Department of Land Resources and Environmental Sciences, Montana State University, Bozeman, Montana

<sup>4</sup>College of Earth, Ocean, and Atmospheric Sciences, Oregon State University, Corvallis, Oregon

<sup>5</sup>Department of Earth, Ocean, and Ecological Sciences, School of Environmental Sciences, University of Liverpool, Liverpool, United Kingdom

<sup>6</sup>Ocean Sciences Department, University of California, Santa Cruz, California

### Abstract

We present nearly 9 yrs (June 2005–December 2013) of measurements of upper-ocean (0 m to 125 m) dinitrogen (N<sub>2</sub>) fixation rates, coupled with particulate nitrogen (PN) export at 150 m, from Station ALOHA (22° 45'N, 158°W) in the North Pacific Subtropical Gyre. Between June 2005 and June 2012, N<sub>2</sub> fixation rates were measured based on adding the <sup>15</sup>N<sub>2</sub> tracer as a gas bubble. Beginning in August 2012, <sup>15</sup>N<sub>2</sub> was first dissolved into filtered seawater and the <sup>15</sup>N<sub>2</sub>-enriched water was subsequently added to N<sub>2</sub> fixation incubations. Direct comparisons between methodologies revealed a robust relationship, with the addition of <sup>15</sup>N<sub>2</sub>-enriched seawater resulting in twofold greater depth-integrated rates than those derived from adding a <sup>15</sup>N<sub>2</sub> gas bubble. Based on this relationship, we corrected the initial period of measurements, and the resulting rates of N<sub>2</sub> fixation averaged  $230 \pm 136 \mu\text{mol N m}^{-2} \text{ d}^{-1}$  for the full time series ( $n = 71$ ). Analysis of the <sup>15</sup>N isotopic composition of sinking PN, together with an isotope mass balance model, revealed that N<sub>2</sub> fixation supported 26–47% of PN export during calendar years 2006–2013. The N export derived from these fractional contributions and measured N<sub>2</sub> fixation rates ranged between 502 and 919  $\mu\text{mol N m}^{-2} \text{ d}^{-1}$ , which are equivalent to rates of net community production (NCP) of 1.5 to 2.7  $\text{mol C m}^{-2} \text{ yr}^{-1}$ , consistent with previous independent estimates of NCP at this site.

Nitrogen (N) is a fundamental nutrient for all organisms, required for the synthesis of numerous biomolecules, and its availability and supply often limits productivity and accumulation of plankton biomass in large regions of the world's oceans (Eppley and Peterson 1979; Moore et al. 2013). Supply of bioavailable N to the well-lit regions of the open ocean can occur through a suite of biotic and abiotic processes that include atmospheric deposition, upwelling, turbulent (eddy) diffusion, horizontal and vertical advection, and microbial dinitrogen (N<sub>2</sub>) fixation (Galloway et al. 2004; Karl

et al. 2008). These processes supply exogenous fixed N to the upper ocean, and hence constitute “new” sources of bioavailable N to these ecosystems (Dugdale and Goering 1967). Under steady state, the supply of new N to the euphotic zone should balance N removal, principally through the export of particulate organic N (Eppley and Peterson 1979).

Biological N<sub>2</sub> fixation, the process by which N<sub>2</sub> is reduced to ammonia (NH<sub>3</sub>) by N<sub>2</sub>-fixing microbes (termed diazotrophs), constitutes an important component of new N supply to ocean ecosystems (Capone et al. 2005), thereby fueling the export of carbon (Karl et al. 2012). At Station ALOHA (A Long-term Oligotrophic Habitat Assessment; 22° 45'N, 158° 00'W), the field site of the Hawai'i Ocean Time-series (HOT) program, the supply of fixed N by N<sub>2</sub> fixation has been estimated to be comparable in magnitude to the delivery of new N via mixing, upwelling and/or advection (Karl et al. 1997; Dore et al. 2002). Station ALOHA is home

\*Correspondence: [mjchurch@hawaii.edu](mailto:mjchurch@hawaii.edu)

This is an open access article under the terms of the Creative Commons Attribution-NonCommercial-NoDerivs License, which permits use and distribution in any medium, provided the original work is properly cited, the use is non-commercial and no modifications or adaptations are made.

to metabolically, morphologically, and genetically diverse assemblages of diazotrophs (Zehr and Kudela 2011; Church and Böttjer 2013; Thompson and Zehr 2013). These include at least two genera of unicellular cyanobacteria (the uncultivated *Candidatus Atelocyanobacterium thalassa* and various clades of *Crocosphaera*) and filamentous cyanobacteria (members of the non-heterocystous genus *Trichodesmium* and heterocystous cyanobacteria belonging to the genera *Richelia* and *Calothrix*). Previous studies in the North Pacific Subtropical Gyre (NPSG) indicate that small ( $< 10 \mu\text{m}$ ), presumably unicellular diazotrophs can be important contributors to  $\text{N}_2$  fixation in this ecosystem (Dore et al. 2002; Montoya et al. 2004; Church et al. 2009).

The two most common methodologies used for estimating rates of  $\text{N}_2$  fixation in aquatic systems are acetylene reduction (AR) and  $^{15}\text{N}_2$  assimilation (Capone 1993; Montoya et al. 1996). The AR assay measures the reduction of acetylene to ethylene, a proxy measurement for gross rates of  $\text{N}_2$  fixation. In the open sea where the biomass of  $\text{N}_2$ -fixing microorganisms and rates of  $\text{N}_2$  fixation tend to be low, the sensitivity of the AR method often requires pre-concentrating diazotroph biomass (e.g., Capone et al. 2005) although recent improvements in the sensitivity of this methodology (Wilson et al. 2012) may broaden its application for studies in the open ocean. The  $^{15}\text{N}_2$  assay, which measures the net assimilation of  $^{15}\text{N}_2$  into plankton biomass, was introduced as a direct measure of rates of  $\text{N}_2$  fixation (Montoya et al. 1996). Historically, this methodology relied on injection of  $^{15}\text{N}_2$  gas into a seawater sample followed by an incubation period. However, recent reports indicate that variability in the rate of  $^{15}\text{N}_2$  gas dissolution and the degree of isotope enrichment of the seawater during the incubation period may result in significant underestimation of  $\text{N}_2$  fixation rates by this approach (Mohr et al. 2010; Großkopf et al. 2012; Wilson et al. 2012). Moreover, contamination of commercial  $^{15}\text{N}_2$  gas stocks with  $^{15}\text{N}$ -ammonia ( $\text{NH}_3$ ) and  $^{15}\text{N}$ -nitrogen oxides ( $\text{NO}_x$ ) has recently been reported, further complicating use of the  $^{15}\text{N}_2$  methodology (Dabundo et al. 2014).

Assuming balance in N supply and export to the deep ocean, assessment of the proportion of naturally occurring N isotopes in sinking organic matter can also be useful for constraining the relative importance of different N substrates in supporting new production (Wada and Hattori 1976). The proportion of  $^{15}\text{N}$  relative to  $^{14}\text{N}$  is frequently expressed using the  $\delta^{15}\text{N}$  notation (‰ deviation from the  $^{15}\text{N} : ^{14}\text{N}$  ratio of atmospheric  $\text{N}_2$ , which by definition has a  $\delta^{15}\text{N}$  of 0‰). Deep ocean (300–1500 m) nitrate ( $\text{NO}_3^-$ ) has an enriched  $\delta^{15}\text{N}$  signature ranging between  $\sim 5.5\text{‰}$  and  $8.9\text{‰}$  (Casciotti et al. 2008; Sigman et al. 2009) while the  $\delta^{15}\text{N}$  signature of dissolved  $\text{N}_2$  is  $0.1\text{--}0.6\text{‰}$ , owing to a small equilibrium isotopic fractionation between the dissolved and gaseous phases (Bauersachs et al. 2009). Little or no kinetic isotope fractionation occurs during the biological fixation of  $\text{N}_2$ ; hence, diazotroph biomass  $\delta^{15}\text{N}$  typically ranges between  $-2.2\text{‰}$  and  $0.6$

‰ (Saino and Hattori 1987; Carpenter et al. 1997; Bauersachs et al. 2009). Upper ocean suspended particulate matter in the NPSG has a low  $\delta^{15}\text{N}$  signature ( $-1.0\text{‰}$  to  $2.0\text{‰}$ ; Dore et al. 2002), likely reflecting the combined influences of this low  $\delta^{15}\text{N}$  source and kinetic isotopic fractionations associated with intensive recycling of organic matter in this oligotrophic habitat (Checkley and Miller 1989). However, in steady state, the export of organic N from the upper ocean should balance new N supply (Dugdale and Goering 1967; Eppley and Peterson 1979). Assuming  $\text{NO}_3^-$  and  $\text{N}_2$  fixation represent the dominant sources of new N to the upper ocean, the isotopic differences in these two end-member supply terms, together with measured  $\delta^{15}\text{N}$  signatures of sinking particulate nitrogen (PN), are useful proxies for discriminating the relative importance of  $\text{N}_2$  fixation and upward  $\text{NO}_3^-$  transport in providing new N to support organic matter export from the upper ocean (Dore et al. 2002, Knapp et al. 2016).

In the current study, we present nearly 9 yr (June 2005–December 2013) of measurements ( $n = 71$ ) of upper ocean (0–125 m) rates of  $\text{N}_2$  fixation estimated using the  $^{15}\text{N}_2$  methodology. In addition, through analyses of  $\delta^{15}\text{N}$  isotopic signatures of sinking PN collected between 2006 and 2013 from sediment traps deployed at 150 m, we estimate the fractional contribution of  $\text{N}_2$  fixation to the supply of fixed N supporting PN export at this site, thereby constraining the importance of  $\text{N}_2$  fixation as a source of new N to the NPSG ecosystem.

## Methods

### Sample location and collection

Sampling for this study relied on the regular HOT program time-series cruises to Station ALOHA. Seawater samples for subsequent determinations of rates of  $^{15}\text{N}_2$  fixation (2005–2013) and nutrient concentrations (1989–2013) were obtained using a conductivity-temperature-depth rosette sampler equipped with 24 polyvinyl chloride sample bottles. Mixed layer depths (MLD) were calculated based on a threshold change in seawater density of  $0.125 \text{ kg m}^{-3}$  relative to the sea surface. Penetration of photosynthetically active radiation was measured during each HOT cruise at approximately noon using vertically profiling radiometers (PRR 600, Biospherical Instruments, from February 1998 to August 2009; and HyperPro, Satlantic, from September 2009). Sinking particles were collected using a free-floating sediment trap array holding 12 replicate cylindrical particle interceptor traps deployed at 150 m for  $\sim 72 \text{ h}$  (Knauer et al. 1979).

### $^{15}\text{N}_2$ fixation rate estimates

Rates of  $^{15}\text{N}_2$  fixation were measured using the  $^{15}\text{N}_2$  isotopic tracer technique (adapted from Montoya et al. 1996). Whole seawater samples from six discrete depths (5, 25, 45, 75, 100, and 125 m) were subsampled into acid-washed 4.3 L polycarbonate bottles and sealed with caps fitted with silicone septa. Between June 2005 and May 2012, 3 mL of  $^{15}\text{N}_2$

gas (98% from Cambridge Isotope Laboratories between June 2005 and September 2009 or Sigma-Aldrich between November 2009 and May 2012) was injected into each polycarbonate bottle through the septum using a gas-tight syringe fitted with a stainless steel needle. Beginning in August 2012, the  $^{15}\text{N}_2$  gas was first dissolved into seawater (prepared as described in Wilson et al. 2012) and 100 mL of the resulting  $^{15}\text{N}_2$ -enriched water was added to 4.3 L polycarbonate sampling bottles ( $^{15}\text{N}_2$  gas distributed from Sigma-Aldrich between June 2012 and September 2013 and Cambridge Isotope Laboratories between October and December 2013). The atom % enrichment of stocks of  $^{15}\text{N}_2$ -enriched seawater was measured using a membrane inlet mass spectrometer (MIMS; Kana et al. 1994). Nitrogen masses 28, 29, and 30 were quantified from duplicate subsamples of  $^{15}\text{N}_2$ -enriched seawater stocks stored in crimp-sealed 70 mL vials. Masses 32 and 40 were also determined and the resulting  $\text{O}_2 : \text{Ar}$  ratio calculated to evaluate instrument drift during analysis; filtered seawater served as reference material. The atom % enrichment of  $^{15}\text{N}_2$  in the prepared stocks was calculated based on the concentration ( $\mu\text{mol kg}^{-1}$ ) of masses 28, 29, and 30.

Incubation bottles amended with the  $^{15}\text{N}_2$  tracer were attached to a free-drifting array and incubated at the discrete depths from which samples had been collected. The array was deployed before dawn and samples were incubated at *in situ* light and temperature for 24 h (Church et al. 2009). After recovery of the array, the entire volume from each bottle was filtered onto a pre-combusted glass microfiber filter (Whatman 25 mm GF/F). Filters were placed onto pre-combusted pieces of foil in Petri dishes and stored frozen at  $-20^\circ\text{C}$ .

We conducted two experiments (November and December 2014) evaluating how different sources of commercial  $^{15}\text{N}_2$  gas stocks influenced measured rates of  $^{15}\text{N}$  assimilation into plankton biomass, and hence might influence the resulting time-series rates of  $\text{N}_2$  fixation reported in this study. For these experiments, triplicate 4.3 L polycarbonate bottles were filled with surface seawater (5 m) from Station ALOHA, amended with  $^{15}\text{N}_2$ -enriched seawater prepared using  $^{15}\text{N}_2$  gas supplied by two different vendors (98 atom % Sigma-Aldrich lots SZ1670V, EB1169, and CX0937; and 98 atom % Cambridge Isotope Laboratories lot I-16727), and incubated for 24 h in a shaded, surface seawater-cooled deck-board incubator. At the end of the incubation, the entire volume of each bottle was filtered onto pre-combusted glass microfiber filters (Whatman GF/F) and filters were processed as previously described.

In four additional experiments, conducted in July and August 2011 (Wilson et al. 2012), September 2012, and November 2014, we compared  $\text{N}_2$  fixation rates derived from adding  $^{15}\text{N}_2$  in gaseous or dissolved form. For these experiments, six 4.3 L polycarbonate bottles each were filled with seawater collected from three discrete depths (5, 25, and 45 m). Triplicate bottles were spiked with either 3 mL of  $^{15}\text{N}_2$  gas (from Sigma-Aldrich in September 2012 and

Cambridge in November 2014) or 100 mL  $^{15}\text{N}_2$ -enriched water as described above. After capping, the bottles were attached to a free-drifting array and incubated at *in situ* light and temperature for 24 h. Once the array was recovered, bottles were detached and the entire volume from each bottle was filtered onto pre-combusted glass microfiber (Whatman 25 mm GF/F) filters. Filters were placed onto pre-combusted pieces of foil in Petri dishes and stored frozen at  $-20^\circ\text{C}$ .

At the shore-based laboratory, all filters were dried for 24 h at  $60^\circ\text{C}$ , pelleted, and the total mass of N and its isotopic signature ( $\delta^{15}\text{N}$ ) on each filter were analyzed by the Stable Isotope Facility at the University of Hawai'i using an elemental analyzer-isotope ratio mass spectrometer (Carlo-Erba EA NC2500 coupled with ThermoFinnigan Delta S). Rates of  $^{15}\text{N}_2$  fixation were calculated as described in Capone and Montoya (2001). The atom % enrichment in incubations following the  $^{15}\text{N}_2$  gas bubble injection (June 2005–May 2012) was calculated assuming complete isotopic equilibration between the gas bubble and the seawater. For the period where aliquots of  $^{15}\text{N}_2$ -enriched seawater were added to incubations (August 2012 onwards), the atom % enrichment of  $^{15}\text{N}_2$  in the prepared stocks measured with the MIMS was taken into account when calculating the final atom % enrichment in incubations.

### Inorganic nutrient concentrations

Discrete seawater samples for the analyses of soluble reactive phosphorus (SRP) and nitrate plus nitrite ( $\text{NO}_3^- + \text{NO}_2^-$ ) were collected into clean, acid washed 125 mL and 500 mL polyethylene bottles and immediately frozen upright at  $-20^\circ\text{C}$ . High-sensitivity analytical techniques were utilized because nutrient concentrations in the upper ocean ( $< 100$  m) at Station ALOHA are typically at or below the detection limits of standard nutrient analyses methods. Concentrations of  $\text{NO}_3^- + \text{NO}_2^-$  were analyzed using the chemiluminescent method described by Garside (1982) with modifications described by Dore and Karl (1996). Concentrations of SRP were determined using the MAGnesium Induced Coprecipitation assay (Karl and Tien 1992).

### Export of PN

Sinking PN was collected over  $\sim 72$  h on each cruise using free-drifting sediment traps deployed at 150 m. Each trap array consisted of individual collector traps, filled with  $0.2 \mu\text{m}$  filtered surface seawater solution consisting of  $50 \text{ g L}^{-1}$  sodium chloride and 1% (v/v) formalin. On recovery, six replicate traps were pre-screened through  $335 \mu\text{m}$  Nitex mesh (to remove zooplankton “swimmers”) prior to filtration onto 25-mm diameter combusted glass microfiber filters (Whatman GF/F). These filters were subsequently dried for 24 h at  $60^\circ\text{C}$ , pelleted and analyzed by the Stable Isotope Facility at the University of Hawai'i for the mass of PN and its stable isotope ( $\delta^{15}\text{N}$ ) composition. The fraction of PN flux supported by  $\text{N}_2$  fixation ( $f_{\text{PN-N}_2}$ ) was calculated based on a two-source mass balance model (Dore et al. 2002):  $f_{\text{PN-N}_2} = (\delta^{15}\text{N} - \delta^{15}\text{N}_{\text{ref}}) / (\delta^{15}\text{N}_{\text{fix}} - \delta^{15}\text{N}_{\text{ref}})$ .



PN -  $\delta^{15}\text{NO}_3^-/(\delta^{15}\text{N}_2 - \delta^{15}\text{NO}_3^-)$ , where  $\delta^{15}\text{N}_2$ ,  $\delta^{15}\text{NO}_3^-$ , and  $\delta^{15}\text{N-PN}$  are the isotopic signatures of newly fixed  $\text{N}_2$ , upwardly transported nitrate and sinking PN, respectively. The fractional contribution of upwardly transported  $\text{NO}_3^-$  to PN export was calculated as  $f_{\text{PN-NO}_3^-} = 1 - f_{\text{PN-N}_2}$ . From the time-integrated mean measured  $\text{N}_2$  fixation rate ( $F_{\text{N}_2}$ ), fluxes of  $\text{NO}_3^-$  ( $F_{\text{NO}_3^-}$ ) and sinking PN ( $F_{\text{PN}}$ ) were estimated as:  $F_{\text{NO}_3^-} = (f_{\text{PN-NO}_3^-}/f_{\text{PN-N}_2}) \times F_{\text{N}_2}$  and  $F_{\text{PN}} = F_{\text{N}_2}/f_{\text{PN-N}_2}$ , respectively. A sensitivity analysis was conducted to constrain the ranges of plausible isotopic end-members; a series of discrete values for  $\delta^{15}\text{N}_2$  (-1.0, 0.0, and 0.6‰) and  $\delta^{15}\text{NO}_3^-$  (3.5, 4.0, 5.0, 6.0, 6.5, and 7.5‰) were selected. Based on the time-integrated average  $\delta^{15}\text{N}$  signature of the sinking PN (3.46‰), the fraction of PN export supported by either  $\text{N}_2$  fixation or  $\text{NO}_3^-$  was derived for the various possible end-member isotopic scenarios.

### Sea surface height anomaly

A combined data product of weekly sea surface height anomalies (SSHA) derived from the TOPEX Poseidon, ERS and Jason-1 satellites was utilized to examine mesoscale physical variability in the vicinity of Station ALOHA between June 2006 and June 2013. The SSHA data product was obtained from the Asia-Pacific Data-Research Center of the International Pacific Research Center ([http://apdrc.soest.hawaii.edu/datadoc/aviso\\_topex.php](http://apdrc.soest.hawaii.edu/datadoc/aviso_topex.php)).

## Results

### Habitat characteristics at Station ALOHA

Time-resolved sampling at Station ALOHA by the HOT program revealed that the upper ocean experiences moderate seasonal variability in biogeochemistry and hydrographic forcing. During the cooler fall and winter months (November through April), sea surface temperatures typically range between 23.4°C and 25.5°C, MLD averages  $73 \pm 14$  m, incident irradiance ranges between 24 and 47 mol quanta  $\text{m}^{-2} \text{d}^{-1}$ , and depth integrated N + N inventories in the lower euphotic zone (75–125 m) often exceed 8 mmol N  $\text{m}^{-2}$  (Fig. 1; Table 1). Through the late spring, summer, and early fall (May–October), sea surface temperatures increase (ranging between 24.4°C and 26.4°C), the upper ocean becomes progressively more stratified (the mixed layer typically shoals to  $\leq 60$  m), incident irradiance often exceeds 45 mol quanta  $\text{m}^{-2} \text{d}^{-1}$ , and depth-integrated N + N inventories between 75 m and 125 m are  $< 4$  mmol N  $\text{m}^{-2}$  (Fig. 1; Table 1). Upper euphotic zone N + N inventories ( $< 45$  m) are relatively constant throughout the year (Fig. 1c), and hence seasonality in euphotic zone  $\text{NO}_3^- + \text{NO}_2^-$  inventories is largely controlled by variations in the depth of nitracline (Letelier et al. 2004). The molar  $\text{NO}_3^- + \text{NO}_2^-$  : SRP ratios of the depth-integrated (0–125 m) nutrient inventories remain  $< 2$ , well below the canonical Redfield ratio (16N : 1P; Table 1).

### Time-series rate measurements of $\text{N}_2$ fixation

Time-series rates of  $\text{N}_2$  fixation were assessed on a near-monthly basis between June 2005 and December 2013. Assimilation of  $^{15}\text{N}_2$  gas into plankton biomass provided insight into the vertical and temporal variability associated with the diazotroph activity in this ecosystem. Between June 2005 and May 2012, these rate measurements relied on the addition of  $^{15}\text{N}_2$  as a gas bubble, whereas between August 2012 and December 2013 the  $^{15}\text{N}_2$  tracer was first dissolved in 0.2  $\mu\text{m}$  filtered seawater and the resulting  $^{15}\text{N}_2$ -enriched seawater was added to each sample for the subsequent incubation. The atom % enrichment of the seawater stocks utilized for the enriched seawater tracer addition ranged between 74% and 81%, averaging  $79 \pm 2\%$ , which resulted in a final atom % enrichment between 2.8% and 3% in the seawater incubations. Vertical profiles throughout the study period showed that the majority ( $67 \pm 12\%$ ) of  $^{15}\text{N}_2$  fixation occurred in the upper region of the water column (Fig. 2). Depth-integrated rates of  $^{15}\text{N}_2$  fixation in the well-lit part of the euphotic zone (0–45 m) ranged between 11 and 271  $\mu\text{mol N m}^{-2} \text{d}^{-1}$  and were significantly greater than those in the lower regions of the euphotic zone (75–125 m), which varied from 6 to 114  $\mu\text{mol N m}^{-2} \text{d}^{-1}$  (one-way ANOVA,  $p < 0.001$ ).

Depth-integrated (0–125 m) rates of  $^{15}\text{N}_2$  fixation between June 2005 and May 2012 ranged between 16 and 347  $\mu\text{mol N m}^{-2} \text{d}^{-1}$ , with rates varying fourfold to ninefold over the course of the year (Fig. 3). Rates of  $^{15}\text{N}_2$  fixation during the latter period (August 2012–December 2013), when  $^{15}\text{N}_2$  was added as enriched seawater, ranged between 23 and 448  $\mu\text{mol N m}^{-2} \text{d}^{-1}$  and were significantly greater (one-way ANOVA,  $p < 0.05$ ) than rates measured during the initial period of the time series. Direct comparisons between adding  $^{15}\text{N}_2$  in gaseous vs. dissolved form conducted on four separate occasions (July 2011, August 2011, September 2012, and November 2014) revealed a robust linear relationship between the two methodologies as used in this study (Fig. 4). The addition of  $^{15}\text{N}_2$ -enriched seawater yielded systematically greater (approximately twofold) rates of  $^{15}\text{N}_2$  fixation than those derived when the  $^{15}\text{N}_2$  tracer was added as a bubble (Fig. 4). Since we utilized the same incubation protocols and procedures (i.e., *in situ* incubations, consistency in length of incubation, identical volumes of  $^{15}\text{N}_2$  gas tracer and seawater) and the upper ocean undergoes only modest seasonal changes in temperature and salinity (minimizing variability in the solubility of  $^{15}\text{N}_2$ ), we utilized the empirical relationship between the bubble and dissolved methodologies to compute revised rates of  $^{15}\text{N}_2$  fixation for the initial period (June 2005–June 2013) of  $^{15}\text{N}_2$  measurements. The resulting rates of  $\text{N}_2$  fixation for the full time series ranged between 21 and 676  $\mu\text{mol N m}^{-2} \text{d}^{-1}$  (averaging  $230 \pm 136$   $\mu\text{mol N m}^{-2} \text{d}^{-1}$ ).

Rates of  $^{15}\text{N}_2$  fixation were most variable, but generally elevated, during periods when the upper ocean at Station

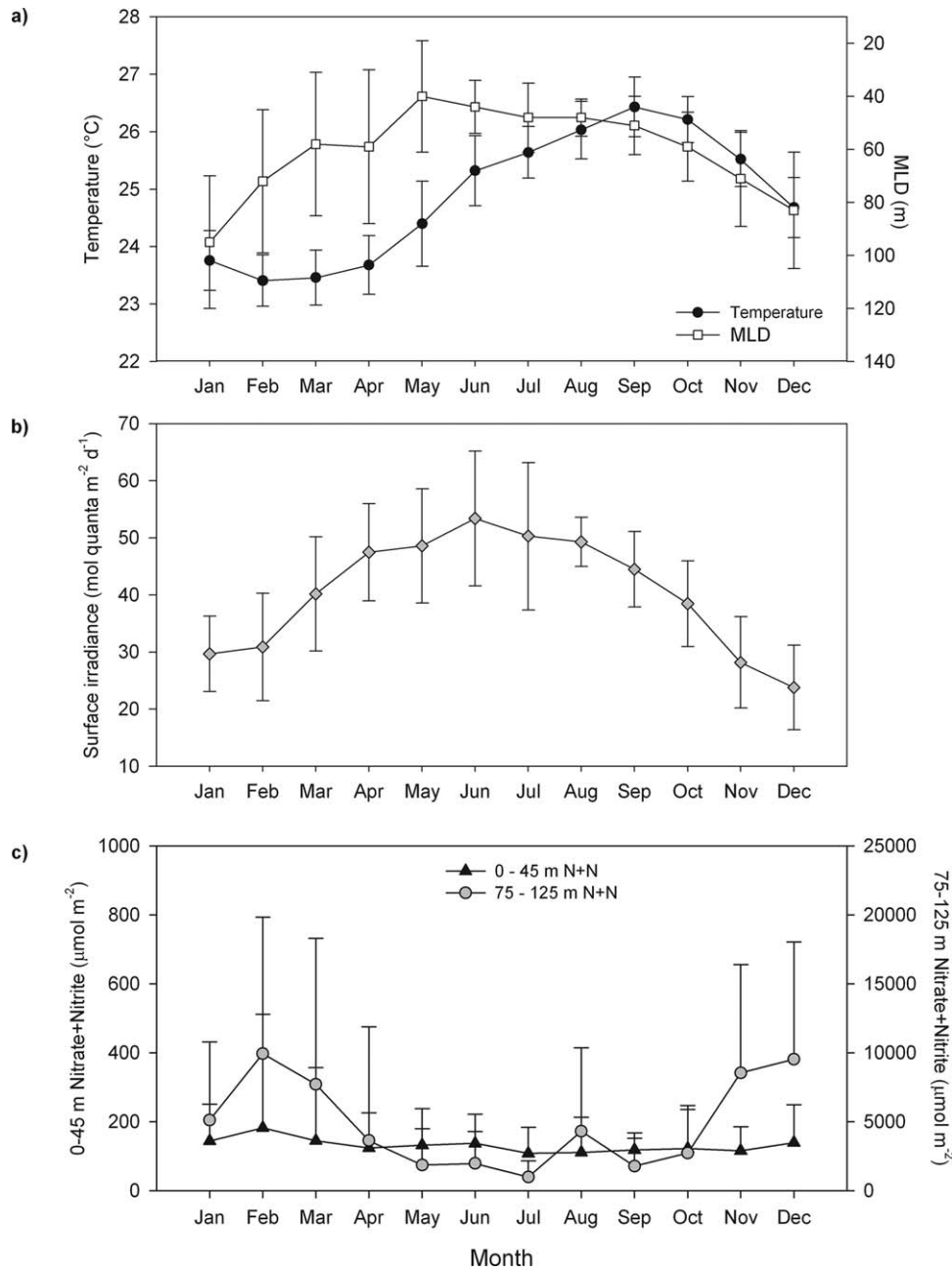


**Fig. 1.** Monthly binned near-surface ocean temperatures and mixed layer depths (MLD; panel **A**), surface irradiance (panel **B**), and nitrate + nitrite (N + N) inventories (panel **C**) at Station ALOHA between 1989 and 2013 (irradiance measurements between 1998 and 2009). N + N inventories are depth integrated from 0 m to 45 m and 75 m to 125 m. Vertical error bars represent standard deviation of the monthly means.

ALOHA was warm and stratified (Fig. 5, Table 2), with rates between May and October often exceeding  $200 \mu\text{mol N m}^{-2} \text{d}^{-1}$  (averaging  $263 \pm 147 \mu\text{mol N m}^{-2} \text{d}^{-1}$ ). Periods of elevated  $^{15}\text{N}_2$  fixation tended to coincide with periods when the upper ocean was warm and satellite-derived SSHA were positive, ranging between 3 cm and 19 cm (Fig. 6). In comparison, rates of  $^{15}\text{N}_2$  fixation measured between the months of November through April, when the upper ocean was cooler and less stratified, were significantly (one-way ANOVA,

$p < 0.01$ ) lower (generally  $\leq 200 \mu\text{mol N m}^{-2} \text{d}^{-1}$ ) compared to May through October.

During the course of this study, we utilized  $^{15}\text{N}_2$  gas supplied from two different vendors: Cambridge Isotope Laboratories, (June 2005–September 2009 and October–December 2013) and Sigma-Aldrich (November 2009–September 2013). A recent report (Dabundo et al. 2014) measured varying levels of  $^{15}\text{NH}_3$  and  $^{15}\text{NO}_x$  as contaminants in commercially available  $^{15}\text{N}_2$  gases, including those supplied by the vendors

**Table 1.** Mean monthly depth-integrated (0 m to 125 m) nutrient inventories and elemental ratios at Station ALOHA. N + N = nitrate + nitrite;  $\mu\text{mol m}^{-2}$ , SRP = soluble reactive phosphorus ( $\mu\text{mol m}^{-2}$ ).

	JAN	FEB	MAR	APR	MAY	JUN	JUL	AUG	SEP	OCT	NOV	DEC	Significance
N+N	5601 $\pm$ 5833	10468 $\pm$ 10147	8335 $\pm$ 10825	3836 $\pm$ 9196	2336 $\pm$ 2781	2318 $\pm$ 2476	1163 $\pm$ 1154	4845 $\pm$ 6265	2105 $\pm$ 2139	3090 $\pm$ 3267	8854 $\pm$ 8032	10024 $\pm$ 9616	***
SRP	6342 $\pm$ 2539	7206 $\pm$ 3825	7605 $\pm$ 3789	8517 $\pm$ 3162	7470 $\pm$ 3977	6948 $\pm$ 2980	7017 $\pm$ 3479	8714 $\pm$ 4621	7547 $\pm$ 4759	5805 $\pm$ 3489	6876 $\pm$ 3017	7342 $\pm$ 2705	ns
N+N:SRP	1.0 $\pm$ 1.0	1.7 $\pm$ 1.6	1.2 $\pm$ 1.4	0.4 $\pm$ 0.8	0.4 $\pm$ 0.5	0.4 $\pm$ 0.4	0.2 $\pm$ 0.2	0.7 $\pm$ 0.8	0.4 $\pm$ 0.4	0.7 $\pm$ 0.6	1.4 $\pm$ 1.1	1.6 $\pm$ 1.5	***

Significance levels: ns =  $p > 0.05$ , \*\*\* =  $p > 0.001$ .

utilized for the current study. For this reason we conducted two field experiments comparing rates of  $^{15}\text{N}_2$  fixation based on use of  $^{15}\text{N}_2$ -enriched seawater prepared using three different batches of  $^{15}\text{N}_2$  gas from Sigma-Aldrich (lots CX0937, EB1169, and SZ1670V) and one batch from Cambridge Isotope Laboratories (lot I-16727; Fig. 7a,b). In these experiments, utilization of  $^{15}\text{N}_2$  gas supplied by Cambridge resulted in rates of  $^{15}\text{N}_2$  fixation that were not significantly different (one-way ANOVA,  $p > 0.05$ ) of than those derived using Sigma-Aldrich lots CX0937 and EB1169  $^{15}\text{N}_2$  gas (Fig. 7). Moreover, rates of  $^{15}\text{N}_2$  fixation measured *in situ* during these same cruises (HOT 267 and 268) using  $^{15}\text{N}_2$ -enriched seawater prepared with  $^{15}\text{N}$  gas from Cambridge Isotope Laboratories  $^{15}\text{N}_2$  gas (lot I-16727) were comparable (Fig. 7). In contrast, rates of  $^{15}\text{N}_2$  fixation were significantly greater when using  $^{15}\text{N}_2$ -enriched seawater prepared from the Sigma-Aldrich lot# SZ1670 (one-way ANOVA,  $p < 0.001$ ; Fig. 7a,b). Similarly, rates of  $^{15}\text{N}_2$  fixation measured *in situ* during these cruises using  $^{15}\text{N}$  gas supplied from Sigma-Aldrich (lot SZ1670), were considerably greater than the time-averaged rates of  $^{15}\text{N}_2$  fixation measured over the course of this time-series (Fig. 7). As a result, we assumed these anomalously high rates resulted from contamination of the  $^{15}\text{N}_2$  gas, and excluded these measurements from all analyses in this study.

#### Total PN flux and sources supporting PN export

Sediment trap-based export of PN at 150 m during the period of this study (2005–2013) ranged between 80 and 510  $\mu\text{mol N m}^{-2} \text{ d}^{-1}$  (averaging  $279 \pm 86 \mu\text{mol N m}^{-2} \text{ d}^{-1}$ ; Fig. 3a). PN export was typically elevated ( $> 350 \mu\text{mol N m}^{-2} \text{ d}^{-1}$ ) in the summer (between May and August), with lower fluxes ( $\leq 300 \mu\text{mol N m}^{-2} \text{ d}^{-1}$ ) during the remainder of the year (Table 2; one-way ANOVA,  $p < 0.001$ ). No significant seasonality was detected in the  $\delta^{15}\text{N}$  signature of the PN export (one-way ANOVA,  $p > 0.05$ ; Table 2).

Assuming  $\text{N}_2$  fixation and vertical input of  $\text{NO}_3^-$  were the only sources of new N to the upper ocean, we utilized a two end-member N source model to estimate the relative contribution of  $\text{NO}_3^-$  and  $\text{N}_2$  fixation to PN export over an 8-yr time scale (2006–2013; Table 3). Based on measurements of the  $\delta^{15}\text{N}$  composition of the sinking PN flux during this study, together with the direct measurements of  $^{15}\text{N}_2$  fixation, we performed a sensitivity analysis to constrain the  $\delta^{15}\text{N}$  end-member values of the N sources (Table 3). For this analysis, we evaluated end-member signatures for  $\text{N}_2$  fixation ranging between  $-1.0\text{‰}$  and  $0.6\text{‰}$  and  $\text{NO}_3^-$  end-member signatures ranging from  $3.5\text{‰}$  to  $7.5\text{‰}$  (Table 3). These ranges are consistent with measured  $\delta^{15}\text{N}$  signatures of diazotroph biomass (Saino and Hattori 1987; Carpenter et al. 1997; Bauersachs et al. 2009) and measurements of  $\delta^{15}\text{NO}_3^-$  from vertical profiles in the subtropical North Pacific (Casciotti et al. 2008; Mahaffey et al. 2008; Sigman et al. 2009), respectively. We constrained our selection of realistic  $\delta^{15}\text{N}$  values for subsequent analysis by comparing our direct

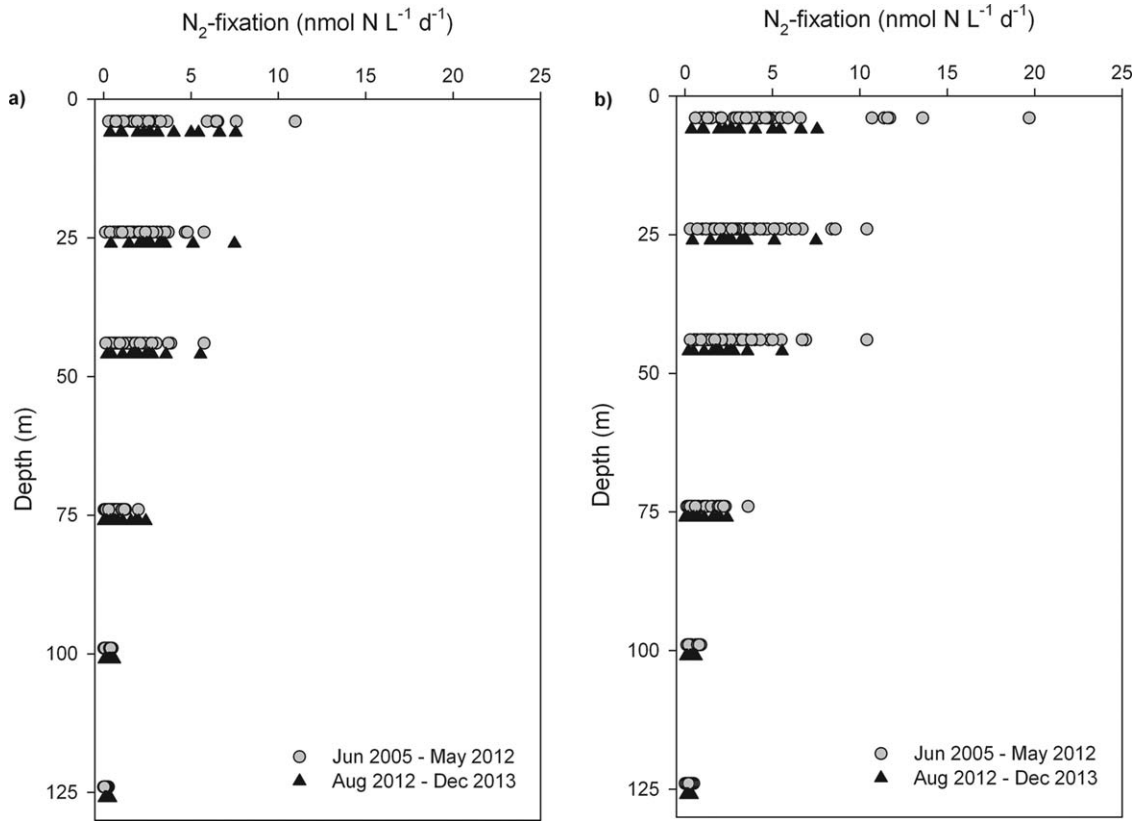


**Fig. 2.** Vertical depth profile (0 m to 125 m) showing volumetric rates of  $N_2$  fixation measured at Station ALOHA between June 2005 and December 2013. Symbols depict the two periods of varying addition of  $^{15}N_2$ : gray circles = addition of a  $^{15}N_2$  gas bubble ( $^{15}N_2$  fixation<sub>Bubble</sub>); black triangles = addition of  $^{15}N_2$ -enriched seawater. Rate measurements during the initial period (June 2005–May 2012;  $^{15}N_2$  fixation<sub>Bubble</sub>) are presented before (panel **A**) and after (panel **B**) correcting for the methodological underestimation using the empirical relationship shown in Fig. 4a.

measurements of  $F_{PN}$  with those derived from measured  $N_2$  fixation rates and the isotope model (Table 3). Results from this sensitivity analysis yielded reasonable values of modeled  $F_{PN}$  for all tested  $\delta^{15}N_2$  values; however, the lower tested  $\delta^{15}NO_3^-$  values of 4.0‰ and 3.5‰ yielded unreasonable  $F_{PN}$  values 8- and 98-times larger, respectively, than measured  $F_{PN}$  from sediment trap collections.

Reanalyzing the  $\delta^{15}NO_3^-$  data of Casciotti et al. (2008), we find that the  $\delta^{15}N$  signatures of the vertical flux of nitrate at Station ALOHA measured in that study were 7.1‰, 6.4‰, and 5.2‰ at 300, 250, and 200 m depth, respectively. Given that the ventilation timescale of these waters (based on inert gas tracers) is  $\geq$  decadal at 300 m and  $\leq$  annual at 200 m (Bullister et al. 2006), and that nitrate concentrations increase rapidly with depth through this zone, we focus our attention on the waters between about 200 and 250 m as best representing the  $\delta^{15}NO_3^-$  supporting new N production over the 8-yr timescale of our observational period; that is, we consider a  $\delta^{15}NO_3^-$  range of approximately 5–6‰ to best represent the nitrate isotopic end-member. This contention is consistent with the time-series  $NO_3^-$  observations of Johnson et al. (2010), which demonstrated a seasonally recurring deficit of  $NO_3^-$  in the waters from 100 down to 250 m at Station ALOHA.

Based on this range of end-member signatures, we computed the fraction of the measured annual PN flux supported by  $N_2$  fixation and  $NO_3^-$ . The modeled fractional contribution of  $N_2$  fixation to PN export flux ranged from 26% to 47% (Table 3). Assuming the directly measured rates of  $N_2$  fixation (corrected for the “bubble effect”) accurately describe the magnitude of new N input by this process, and utilizing the derived fractional contribution of  $NO_3^-$  from the isotope model, we also estimated the  $NO_3^-$  flux ( $F_{NO_3^-}$ ) into the euphotic zone at Station ALOHA at 266–683  $\mu\text{mol N m}^{-2} \text{ d}^{-1}$ . Similarly, the derived  $F_{PN}$  modeled from measured  $N_2$  fixation rates ranged from 502 to 919  $\mu\text{mol N m}^{-2} \text{ d}^{-1}$  during this study (Table 3).

## Discussion

Despite knowledge that  $N_2$  fixation is an important control on new production, and hence carbon export, in large regions of the open sea, multi-annual time-series measurements of this key biogeochemical process are currently lacking. In the present study, we describe nearly 9 yrs (2005–2013) of repeated measurements of upper ocean (0–125 m) rates of  $N_2$  fixation from Station ALOHA in the NPSG. The



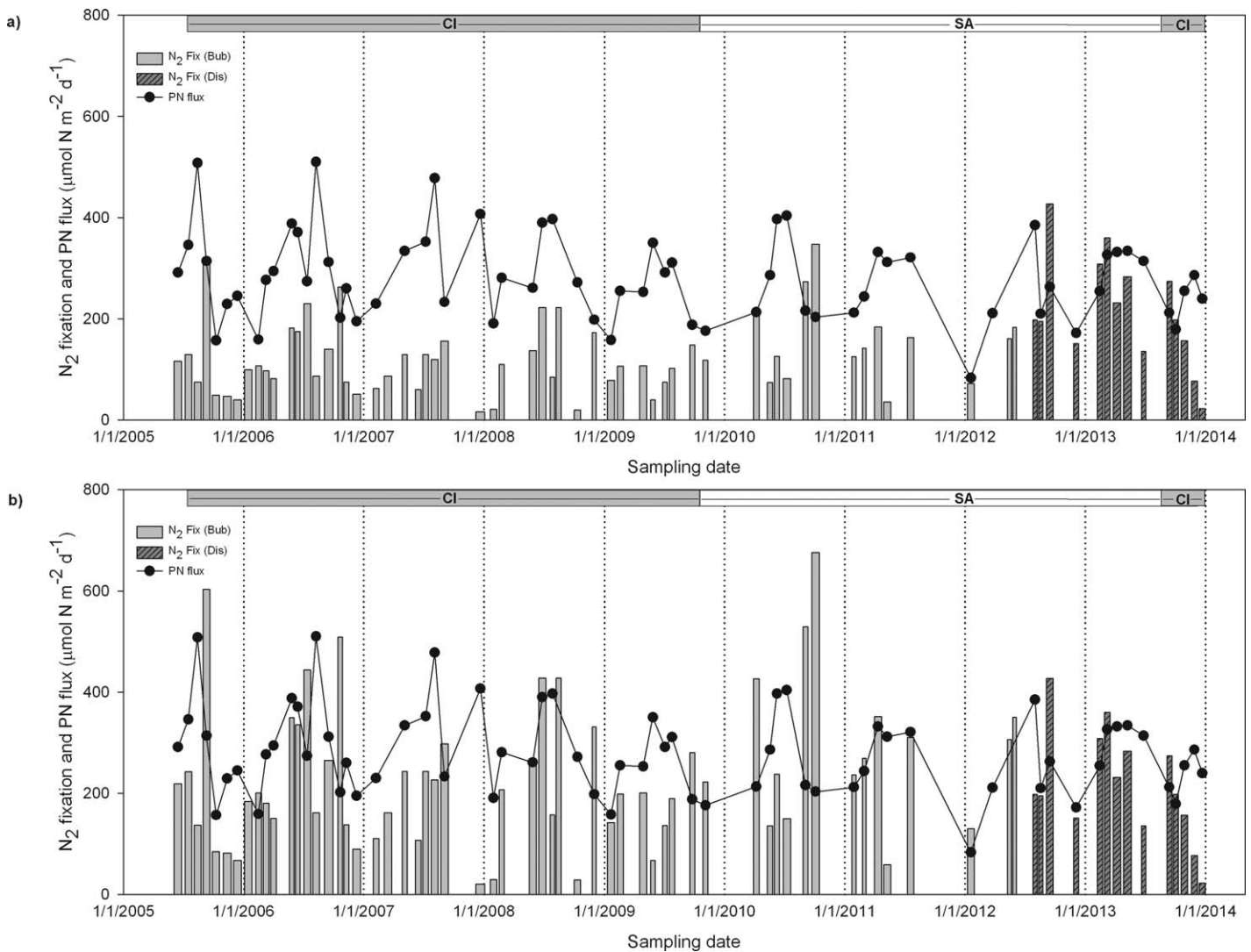


**Fig. 3.** Time series of depth-integrated (0 m to 125 m) rates of  $N_2$  fixation and particulate N export between June 2005 and December 2013 at Station ALOHA. Black line represents the flux of sinking particulate nitrogen (PN) at 150 m. The different colored vertical bars depict the two different methodologies used for the  $^{15}N_2$  measurements; initial period (June 2005–May 2012; light gray bars) are measurements where  $^{15}N_2$  was added as a gas bubble, while latter period (August 2012–December 2013; dark gray bars) depicts measurements where  $^{15}N_2$  tracer was added as enriched seawater. In panel **A**, rate measurements during the initial “bubble” period are shown prior to correcting for the methodological underestimation (see Fig. 4b), whereas panel **B** represents the rate estimates after the correction. CI = Cambridge Isotope, SA = Sigma Aldrich.

resulting time-varying dynamics highlight several important features regarding  $N_2$  fixation in this ecosystem, including: (1) the majority ( $67 \pm 12\%$ ) of  $N_2$  fixation occurs in the well-lit region (0–45 m) of the euphotic zone; (2) during the late summer and early fall months, when the upper ocean is warm and stratified, mesoscale physical processes introduce temporal variability in rates of  $N_2$  fixation; and (3) use of a two-member isotope mass balance model revealed that  $N_2$  fixation supports, on average, 26–47% of the total N export. Taken together, these observations indicate  $N_2$  fixation is an important, albeit time variable, process supplying new N to the upper ocean at Station ALOHA.

Since beginning the  $^{15}N_2$  fixation measurements reported in the current study, there have been a number of methodological challenges identified with the  $^{15}N_2$  tracer methodology. Several recent studies have highlighted the potential for significant underestimation of  $N_2$  fixation rates when  $^{15}N_2$  is added to seawater incubations as a gas bubble (Mohr et al. 2010; Großkopf et al. 2012; Wilson et al. 2012). These studies demonstrate that variability in the time required for the  $^{15}N_2$  gas to reach equilibrium with the seawater relative to the incubation time can result in variability in the  $^{15}N$  atom % enrichment of the seawater. A series of comparative experiments revealed that rates of  $N_2$  fixation derived from the addition of the  $^{15}N_2$  as a gas were 1.7- to 6-fold lower



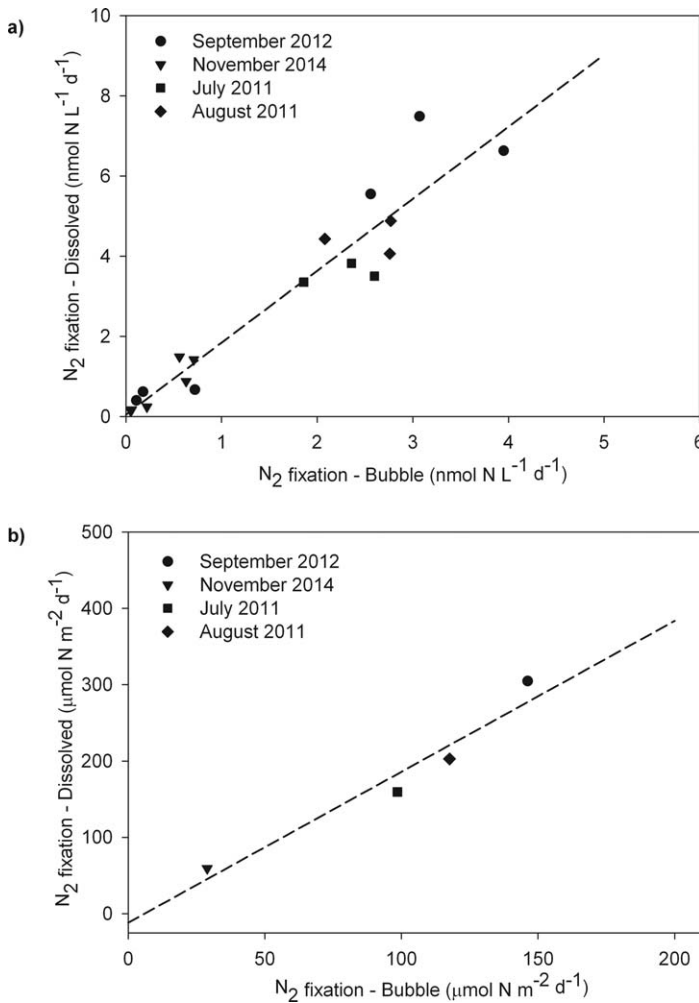


**Fig. 4.** Model II (ordinary least squares) linear regression of volumetric (panel **A**;  $^{15}\text{N}_2 \text{ fixation}_{\text{Dissolved}} = 1.79 \times ^{15}\text{N}_2 \text{ fixation}_{\text{Bubble}} + 0.045$ ;  $r^2 = 0.91$ ,  $p < 0.01$ ) and depth-integrated rates (panel **B**;  $^{15}\text{N}_2 \text{ fixation}_{\text{Dissolved}} = 1.98 \times ^{15}\text{N}_2 \text{ fixation}_{\text{Bubble}} - 11.80$ ;  $r^2 = 0.94$ ,  $p < 0.05$ ) of  $N_2$  fixation measured *in situ* by adding  $^{15}\text{N}_2$  in form of a gas bubble ( $^{15}\text{N}_2 \text{ fixation}_{\text{Bubble}}$ ) vs. adding  $^{15}\text{N}_2$  dissolved as enriched seawater ( $^{15}\text{N}_2 \text{ fixation}_{\text{Dissolved}}$ ). Measurements were conducted in July and August 2011 (reported in Wilson et al. 2012), September 2012, and November 2014.

than rates derived based on the addition of  $^{15}\text{N}_2$  equilibrated with the seawater (Mohr et al. 2010; Großkopf et al. 2012; Wilson et al. 2012). During the initial period of the present study (June 2005–June 2012), we relied on the conventional addition of  $^{15}\text{N}_2$  as a gas bubble. However, beginning in August 2012, we began dissolving the  $^{15}\text{N}_2$  in filtered seawater and adding the  $^{15}\text{N}_2$ -enriched water to the  $N_2$  fixation incubations. The resulting rates of  $N_2$  fixation measured during the latter 1.5-yr period (dissolved addition of  $^{15}\text{N}_2$ ) were significantly greater than those measured during the initial 7.5 yr of measurements, with rates during these two periods averaging  $216 \pm 109$  and  $124 \pm 72 \mu\text{mol N m}^{-2} \text{d}^{-1}$ , respectively. Furthermore, experiments directly comparing both

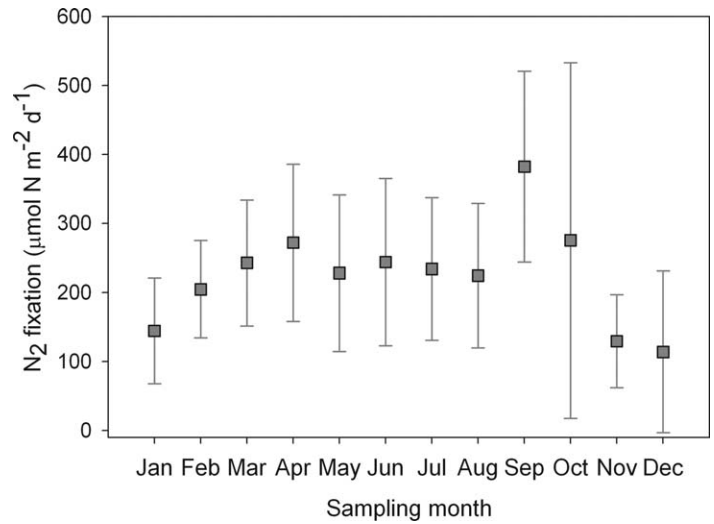


**Fig. 5.** Mean depth-integrated (0 m to 125 m) rates of  $N_2$  fixation binned by month for the period of June 2005–December 2013 with error bars representing one standard deviation of the mean rates. Note: from this figure onwards, measurements during the initial period (June 2005–May 2012) were corrected for apparent methodological underestimation using the empirical relationship described in Fig. 4b.

methodological approaches following the sampling protocols utilized for our time series (24-h incubations on an *in situ* array) revealed a robust relationship between the conventional “bubble” addition and the addition of enriched seawater, with the resulting depth-integrated rates of  $^{15}\text{N}_2$  fixation approximately twofold greater than rates derived from the bubble methodology (Fig. 4). These results are consistent with those of Großkopf et al. (2012) who found that, on average, the enriched seawater approach resulted in a 1.7-fold increase in volumetric rates of  $N_2$  fixation along a meridional transect through the Atlantic Ocean. We followed consistent incubation procedures throughout our time series, except for the mode of introducing  $^{15}\text{N}_2$  gas, including use of *in situ* incubations over 24 h and identical volumes of seawater and  $^{15}\text{N}_2$  tracer. Moreover, the relatively subtle changes in upper ocean temperature (both vertically and seasonally) observed at Station ALOHA likely contributed to the consistent relationship between the “bubble” and “dissolved”  $^{15}\text{N}_2$  incubation methodologies observed in our experiments. We utilized the empirical relationship between rates obtained from these two methodologies to correct the initial period (between June 2005 and May 2012) of the time-series  $N_2$  fixation rates derived using the  $^{15}\text{N}_2$  bubble methodology to account for this methodological underestimation (Table 2).

An additional complication in the  $^{15}\text{N}_2$ -based measurements of  $N_2$  fixation was recently reported in a study by Dabundo et al. (2014) who documented contamination of commercially available  $^{15}\text{N}_2$  gas stocks with  $^{15}\text{N}$ -labeled compounds other than  $^{15}\text{N}_2$ . This study revealed that these contaminants, found in 98 atom %  $^{15}\text{N}$  stocks from Sigma-Aldrich

**Table 2.** Mean monthly particulate nitrogen (PN) export ( $\mu\text{mol N m}^{-2} \text{d}^{-1}$ ) at 150 m, isotopic signature of sinking PN, and depth-integrated (0 m to 125 m) rates of  $^{15}\text{N}_2$  fixation ( $\mu\text{mol N m}^{-2} \text{d}^{-1}$ ) at Station ALOHA.

	JAN	FEB	MAR	APR	MAY	JUN	JUL	AUG	SEP	OCT	NOV	DEC	Significance
Jun 2005–May 2012													
PN export flux	184 $\pm$ 71	231 $\pm$ 52	244 $\pm$ 33	273 $\pm$ 51	353 $\pm$ 70	362 $\pm$ 48	337 $\pm$ 47	484 $\pm$ 30	253 $\pm$ 57	234 $\pm$ 70	230 $\pm$ 38	241 $\pm$ 84	***
$\delta^{15}\text{N}$ of PN	3.6 $\pm$ 0.4	2.7 $\pm$ 0.6	3.6 $\pm$ 0.4	4.1 $\pm$ 0.9	3.3 $\pm$ 0.7	3.3 $\pm$ 0.5	3.4 $\pm$ 0.7	2.5 $\pm$ 1.1	3.3 $\pm$ 0.7	3.4 $\pm$ 1.1	3.5 $\pm$ 1.0	3.9 $\pm$ 1.1	ns
$^{15}\text{N}_2$ fixation	79 $\pm$ 39	96 $\pm$ 23	109 $\pm$ 29	148 $\pm$ 65	118 $\pm$ 60	140 $\pm$ 62	124 $\pm$ 52	126 $\pm$ 67	205 $\pm$ 80	170 $\pm$ 160	80 $\pm$ 36	70 $\pm$ 70	ns
$^{15}\text{N}_2$ fixation†	145 $\pm$ 77	179 $\pm$ 46	204 $\pm$ 58	282 $\pm$ 129	221 $\pm$ 119	265 $\pm$ 122	234 $\pm$ 103	238 $\pm$ 132	395 $\pm$ 159	324 $\pm$ 318	147 $\pm$ 70	127 $\pm$ 139	ns
Aug 2012–Dec 2013													
PN export flux	—	174	186	239	265	306	—	298 $\pm$ 123	279 $\pm$ 23	233 $\pm$ 9	116	150 $\pm$ 31	NA
$\delta^{15}\text{N}$ of PN	—	3.6	4.6	3.3	4.7	4.4	—	3.2 $\pm$ 1.0	3.8 $\pm$ 1.2	3.6 $\pm$ 1.1	4.0	3.4 $\pm$ 0.06	NA
$^{15}\text{N}_2$ fixation	—	308	360	231	283	136	—	197 $\pm$ 2	350 $\pm$ 108	177 $\pm$ 29	77	87 $\pm$ 91	NA

†Depth-integrated monthly means were corrected for methodological underestimation based on the empirical relationship  $^{15}\text{N}_2 \text{ fixation}_{\text{Dissolved}} = 1.98 \times (^{15}\text{N}_2 \text{ fixation}_{\text{Bubble}}) - 11.80$ ; see text for details.

Significance levels: ns =  $p > 0.05$ , \*\*\* =  $p > 0.001$ . NA = statistical test not applicable.

(Isotech Stable Isotopes, lots SZ1670V and MBBB0968V), Cambridge Isotope Laboratories (lot I1-11785A), and Campro Scientific (lot # EB1169V) could result in inflation or false detection of  $^{15}\text{N}_2$  fixation rates (Dabundo et al. 2014). Their study reported relatively low-level contamination of the  $^{15}\text{N}_2$  stocks supplied by Cambridge and Campro Scientific, but significant contamination in stocks obtained from Sigma-Aldrich. During the approximately 9-yr time series reported in the present study,  $^{15}\text{N}_2$  gas stocks purchased from both Cambridge and Sigma-Aldrich were utilized (June 2005–September 2009: Cambridge; November 2009–September 2013: Sigma-Aldrich; October 2013–December 2013: Cambridge Isotope Laboratories); hence, possible  $^{15}\text{N}$ -labeled contaminants introduced with these gases may have influenced our  $^{15}\text{N}_2$  fixation rate measurements. Based on estimated levels of  $\text{NH}_4^+$  contamination reported by Dabundo et al. (2014;  $\sim 25$  to  $1900 \mu\text{mol } ^{15}\text{NH}_4^+$  per mole  $^{15}\text{N}_2$ ), assuming  $\text{NH}_4^+$  concentrations in the upper ocean at Station ALOHA are  $< 0.03 \mu\text{mol L}^{-1}$  (Beman et al. 2012), and that all of the contaminated  $^{15}\text{NH}_4^+$  was consumed during the incubation period, the inferred rate of  $\text{N}_2$  fixation due to  $^{15}\text{NH}_4^+$  contamination would range between  $\sim 0.4$  and  $27 \text{ nmol L}^{-1} \text{d}^{-1}$ . With an average rate of  $\text{N}_2$  fixation in the near-surface ocean of  $2.5 \pm 1.9 \text{ nmol L}^{-1} \text{d}^{-1}$ , potential contamination could have resulted in  $\sim 15$  to  $\sim 1000\%$  overestimation of the inferred rates of  $^{15}\text{N}_2$  fixation. Assuming equal contamination at all depths and  $^{15}\text{NH}_4^+$  contamination of  $25 \mu\text{mol } ^{15}\text{NH}_4^+$  per mole  $^{15}\text{N}_2$  (as indicated in Dabundo et al. 2014), we estimate the resulting depth-integrated (0–125 m) rates from the present study could have been overestimated by  $26\% \pm 11\%$ .

We conducted field-based experiments (Fig. 7a,b) designed to compare rates of  $^{15}\text{N}$  fixation derived from four different stocks of gases supplied from Cambridge (lot I-16727) and Sigma-Aldrich (lots SZ1670V, EB1169, and CX0937). The measured rate of  $^{15}\text{N}_2$  fixation derived from one of the batches of  $^{15}\text{N}_2$  gas supplied from Sigma-Aldrich (lot SZ1670V) was significantly greater than rates measured from use of the other three

batches of  $^{15}\text{N}$  gas (Cambridge Isotope Laboratories lot I-16727 and Sigma-Aldrich lots CX0937 and EB1169), a finding consistent with the levels of contamination reported in the Dabundo et al. (2014) study for this specific lot of  $^{15}\text{N}_2$  gas. During two occasions in the present study (June 2012 and October 2012), rates of  $^{15}\text{N}_2$  fixation during our time-series approached the magnitude of rates observed using presumably contaminated gas stocks (Fig. 7c). We assume these anomalously high rates of  $\text{N}_2$  fixation reflect contamination of the gas stock and we therefore excluded these measurements from further analyses. We cannot exclude the possibility that some of the  $^{15}\text{N}_2$  gas stocks utilized for our direct measurements of  $^{15}\text{N}_2$  fixation may have been contaminated, resulting in overestimation of the measured rates. However, based on experiments conducted in the current study, and the results of Dabundo et al. (2014), we estimate possible contamination would elevate the depth-integrated  $^{15}\text{N}_2$  fixation rate measurements by no more than  $\sim 25\%$ .

Our study revealed that rates of  $\text{N}_2$  fixation at Station ALOHA appear most variable during the warm, stratified periods of the summer. Daily-scale sampling at Station ALOHA during the month of September using a drifting robotic gene sensor demonstrated highly variable diazotroph population dynamics, with abundances of *Trichodesmium* and the unicellular cyanobacteria *Candidatus Atelocyanobacterium thalassa* varying up to three orders of magnitude over  $< 30 \text{ km}$  and over  $< 2 \text{ d}$  time scales (Robidart et al. 2014). Several studies investigating factors controlling the spatiotemporal variability in diazotrophs and  $\text{N}_2$  fixation have revealed episodic changes may be coupled to mesoscale physical variability (Davis and McGillicuddy 2006; Fong et al. 2008; Church et al. 2009), transport and mixing of biogeochemically distinct water masses (Guidi et al. 2012; Robidart et al. 2014), and the legacy of phosphorus originating from winter mixing (Dore et al. 2008). Analysis of satellite-derived SSHA and depth-integrated rates of  $\text{N}_2$  fixation in the present study revealed that periods when rates of  $^{15}\text{N}_2$  fixation were elevated (defined as  $> 1$  standard deviation of

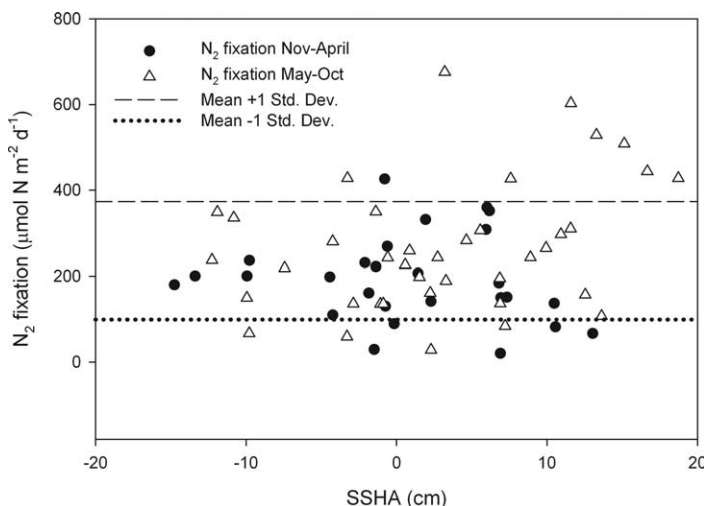


**Fig. 6.** Relationship of depth-integrated (0 m to 125 m) rates of  $\text{N}_2$  fixation and satellite-derived sea surface height anomaly (SSHA) between 2005 and 2013. The two dashed lines depict the  $\pm 1$  standard deviation of the time-integrated mean rate of  $^{15}\text{N}_2$  fixation. Rates of  $^{15}\text{N}_2$  fixation binned into summer and fall and winter and spring months.

the time-averaged rate of  $^{15}\text{N}_2$  fixation) were predominantly associated with positive SSHA (range: 3–19 cm), consistent with the passage of anticyclonic eddies through the study region (Fig. 6). Although such observations have previously been made in the Pacific and Atlantic Ocean (Davis and McGillicuddy; 2006 Fong et al. 2008; Church et al. 2009), the present multi-annual data set highlights that mesoscale physical processes can be important regulators of variability in diazotroph activity at Station ALOHA. Depth-integrated nutrient inventories (0–125 m) measured during these periods of positive SSHA ( $\text{N} + \text{N}$ :  $1578 \pm 1603 \mu\text{mol m}^{-2}$  and  $\text{SRP}$ :  $10,433 \pm 5120 \mu\text{mol m}^{-2}$ ) emphasize that such events coincide with low  $\text{NO}_3^- + \text{NO}_2^-$  :  $\text{SRP}$  ratios, which have been hypothesized to promote the growth of  $\text{N}_2$ -fixing microorganisms (Sohm et al. 2011). Nevertheless, the exact physical, biogeochemical, and ecological processes underlying this apparent mesoscale stimulation of diazotroph activity in the oligotrophic ocean have yet to be identified.

Several key assumptions underlie our use of a two end-member N isotope model to constrain the relative contributions of  $\text{NO}_3^-$  and  $\text{N}_2$  fixation to new production. Specifically, in applying this model we assumed that the euphotic zone N budget was in steady state over annual to subdecadal time scales. Upper ocean nutrient inventories at Station ALOHA have been shown to demonstrate non-steady state dynamics over interannual to subdecadal time scales (e.g., Karl et al. 1997, 2001); however, the magnitude of such variability appears relatively small compared to annual budgets of upper ocean N flux. For example, Hebel and Karl (2001) reported interannual changes in upper ocean (0–150 m) PN inventories of  $< 2 \text{ mmol m}^{-2} \text{ yr}^{-1}$ ; similarly, over subdecadal time scales, inventories of dissolved organic nitrogen (DON)

at Station ALOHA increased at  $\sim 11 \text{ mmol N m}^{-2} \text{ yr}^{-1}$  (Church et al. 2002). However, such changes in upper ocean N pools equate to  $< 10\%$  of the annual new production estimated from this region (Johnson et al. 2010).

In addition, the two end-member isotope model relies on the assumptions that  $\text{N}_2$  fixation and vertical input of  $\text{NO}_3^-$  are the only sources of new N to the upper ocean, and that these sources of new N are balanced by the downward flux of PN. Hence, this approach ignores potential supply of N via atmospheric deposition and/or advection of new N to the upper ocean. Both of these sources are poorly quantified at Station ALOHA; however, supply of N via atmospheric deposition can at times constitute a significant source of N to the upper ocean in some locations (Duce et al. 2008, Kim et al. 2014). A recent analysis on N deposition across the central Pacific Ocean suggested fluxes of N from atmospheric deposition in the region around ALOHA were  $< 10 \text{ mmol N m}^{-2} \text{ yr}^{-1}$ , equivalent to  $< 5\%$  of the new N supply to the upper ocean (Kim et al. 2014). Advection of N into the subtropical gyre is also poorly quantified, but weak north-south gradients in DON concentrations suggest low N supply by this pathway (Abell et al. 2000). Losses of N from the upper ocean can occur through lateral or vertical physical dynamics, sinking particles, or gaseous exchange with the atmosphere. Vertical gradients in DON are  $\sim 10\%$  of the vertical  $\text{NO}_3^-$  gradients (Karl et al. 2001) suggesting downward diffusion of DON could balance only a few percent of the total N supply to the upper ocean (Dore et al. 2002). However, a recent analysis of gradients in dissolved organic carbon and apparent oxygen utilization suggests vertical export of dissolved organic matter could be a significant component of upper ocean export (Emerson 2014). Nitrogen can also be lost from the upper ocean to the atmosphere, whether in the form of  $\text{NH}_3$  or through  $\text{N}_2\text{O}$  production associated with nitrification, denitrification, and nitrifier-denitrification pathways (Dore et al. 1998, Ostrom et al. 2000, Santoro et al. 2011). The upper ocean at Station ALOHA is well oxygenated, so N losses deriving from denitrification are presumed low. Moreover, net fluxes of  $\text{N}_2\text{O}$  from the surface ocean across the air-sea interface at Station ALOHA have been estimated to be between  $0.4$  and  $5.2 \mu\text{mol N m}^{-2} \text{ d}^{-1}$  (Dore et al. 1998), which on the high end would be equivalent to  $\sim 1\%$  of the estimated new production derived in this study. Deposition of N to the surface ocean appears dominated by  $\text{NH}_3$  of marine origin (Jickells et al. 2003, Altieri et al. 2016). Moreover, the flux of  $\text{NH}_3$  from the ocean to the atmosphere in the subtropical gyres also appears low relative to PN export (Paulot et al. 2015). Together, these observations support the notion that sinking particles likely represent the largest loss term by far for new N production in this region.

We utilized a sensitivity analysis of the two end-member isotopic N source model for additional constraint on the contribution of  $\text{N}_2$  fixation to N export at Station ALOHA.

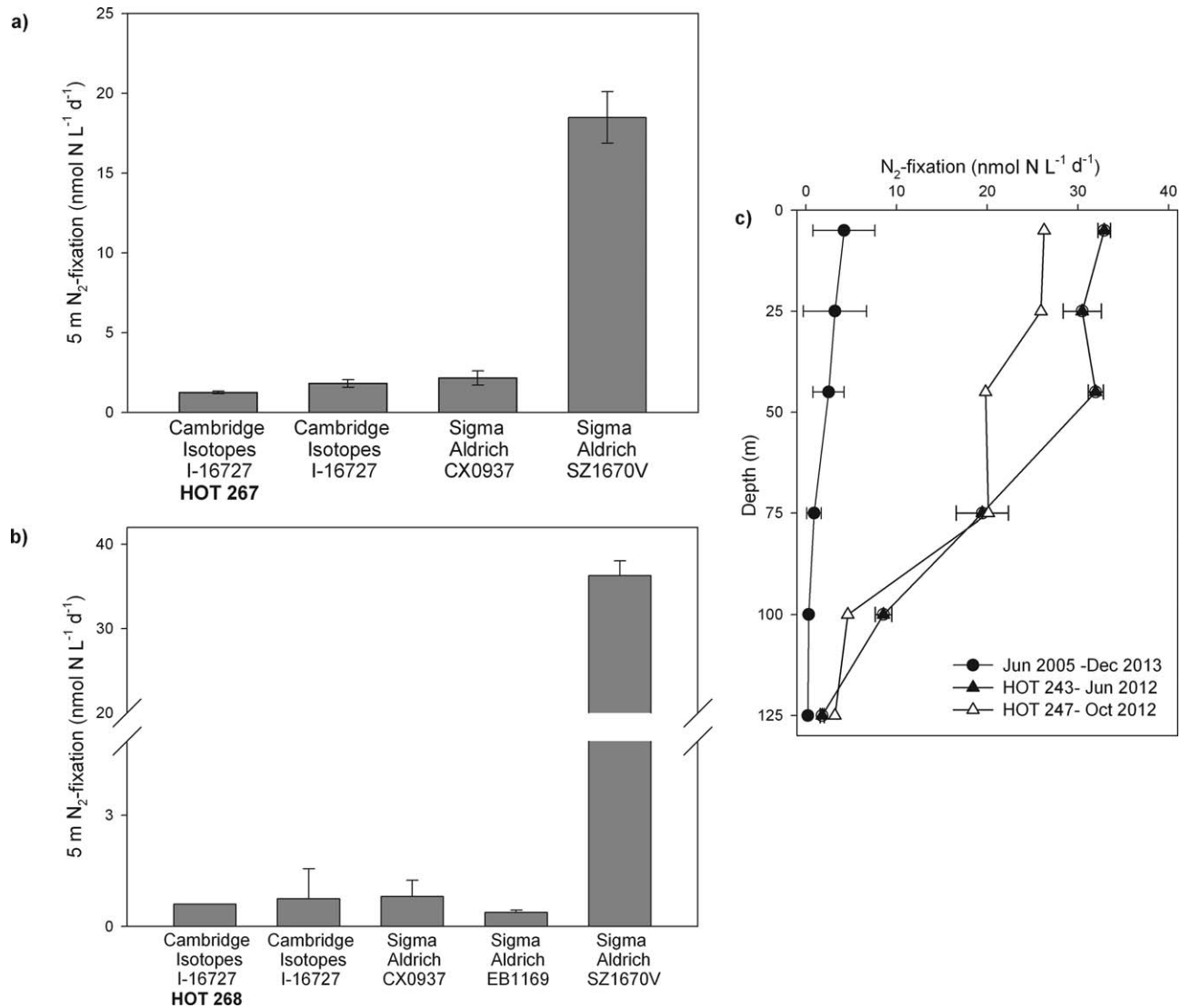


**Fig. 7.** Response of near-surface ocean (5 m)  $N_2$  fixation rates to the enrichment of  $^{15}N_2$  gas distributed by Sigma-Aldrich (lots CX0937, EB1169, and SZ1670V) and Cambridge Isotope Laboratories (lot I-16727) during experiments conducted in November and December 2014 (panel **A** and **B**, respectively). Panel **C** depicts vertical profile of mean volumetric rates of  $^{15}N_2$  fixation measured between June 2005 and December 2013 (black circles), and for two cruises where  $^{15}N_2$  gas appeared contaminated (HOT cruise 243, June 2012, black triangles; and HOT cruise 247, October 2012, open triangles). Vertical and horizontal error bars represent one standard deviation of the mean rates.

While early analyses of subsurface and intermediate waters from the central North Pacific showed  $\delta^{15}N$  values of  $NO_3^-$  averaging close to +6.5‰ (Cline and Kaplan, 1975), a more recent study by Casciotti et al. (2008) suggested a considerably lower  $\delta^{15}N$  signature of  $NO_3^-$  (approximately +3.5‰) near the base of the euphotic zone (150 m) in the study area. To constrain appropriate  $\delta^{15}N$  end-members for the present study, we examined how various permutations of the  $\delta^{15}N$  signatures of  $N_2$  and  $NO_3^-$  influenced the derived contributions of these N sources to PN export (Table 3). Notably, these results revealed that the relatively small variation in the choice of possible  $\delta^{15}N_2$  end-member signature

had minor impact on the fractional contributions of  $N_2$  and  $NO_3^-$ , while the larger possible range in  $\delta^{15}NO_3^-$  end-member values was an important determinant on the magnitude of the derived fluxes. Regardless of the  $\delta^{15}N_2$  end-member signature, use of  $\delta^{15}NO_3^-$  end-members of 3.5 to 4.0‰ resulted in negligible contributions of  $N_2$  fixation to total PN export at Station ALOHA over annual to multi-annual time scales, a finding inconsistent with our nearly 9-yr time series of direct measurements. Moreover, based on this small proportional contribution, and assuming our direct measurements of  $^{15}N_2$  fixation were accurate, use of these low  $\delta^{15}NO_3^-$  end-members yielded unrealistically high N export fluxes (Table 3). In



**Table 3.** Summary of sensitivity analysis of the two end-member model of nitrogen sources supporting particulate nitrogen (PN) export at 150 m at Station ALOHA from 2006 to 2013. The fractions of the PN flux ( $F_{PN}$ ) supported by either  $N_2$  fixation ( $f_{PN-N_2}$ ) or nitrate ( $f_{PN-NO_3^-}$ ) are calculated for several possible combinations of the two isotopic end-members ( $\delta^{15}N_2 = N_2$  fixation and  $\delta^{15}NO_3^- = \text{nitrate}$ ), using the measured time-integrated mean isotopic signature of PN flux ( $\delta^{15}N\text{-PN}$ ). The isotope model is used to estimate the upward flux of nitrate ( $F_{NO_3^-}$ ) and  $F_{PN}$  from the time-integrated mean rate of measured  $N_2$  fixation ( $F_{N_2}$ ). The apparent efficiency of sediment trap collection of PN is calculated as the ratio of measured to modeled  $F_{PN}$ .

$\delta^{15}N_2$ (‰)	$\delta^{15}NO_3^-$ (‰)	$\delta^{15}N\text{-PN}$ (‰)	$f_{PN-N_2}$ (%)	$f_{PN-NO_3^-}$ (%)	$F_{N_2}$ measured ( $\mu\text{mol N m}^{-2} \text{ d}^{-1}$ )	$F_{PN}$ measured ( $\mu\text{mol N m}^{-2} \text{ d}^{-1}$ )	$F_{NO_3^-}$ modeled from $F_{N_2}$ ( $\mu\text{mol N m}^{-2} \text{ d}^{-1}$ )	$F_{PN}$ modeled from $F_{N_2}$ ( $\mu\text{mol N m}^{-2} \text{ d}^{-1}$ )	Apparent trap efficiency (%)
-1.0	3.5	3.46	1	99	236	272	26314	26550	1
-1.0	4.0	3.46	11	89	236	272	1949	2185	12
-1.0	5.0	3.46	26	74	236	272	683	919	30
-1.0	6.0	3.46	36	64	236	272	414	650	42
-1.0	6.5	3.46	41	59	236	272	346	582	47
-1.0	7.5	3.46	48	52	236	272	261	497	55
0.0	3.5	3.46	1	99	236	272	20414	20650	1
0.0	4.0	3.46	14	86	236	272	1512	1748	16
0.0	5.0	3.46	31	69	236	272	530	766	35
0.0	6.0	3.46	42	58	236	272	321	557	49
0.0	6.5	3.46	47	53	236	272	269	505	54
0.0	7.5	3.46	54	46	236	272	202	438	62
0.6	3.5	3.46	1	99	236	272	16874	17110	2
0.6	4.0	3.46	16	84	236	272	1250	1486	18
0.6	5.0	3.46	35	65	236	272	438	674	40
0.6	6.0	3.46	47	53	236	272	266	502	54
0.6	6.5	3.46	52	48	236	272	222	458	59
0.6	7.5	3.46	59	41	236	272	167	403	67

contrast,  $\delta^{15}NO_3^-$  values of between 5.0‰ and 6.0‰ resulted in more realistic proportions of the PN flux supported by  $N_2$  fixation (26% to 47%) and total N fluxes out of the euphotic zone (502–919  $\mu\text{mol N m}^{-2} \text{ d}^{-1}$ ). Also, our modeled  $F_{NO_3^-}$  values ranged from 266 to 683  $\mu\text{mol N m}^{-2} \text{ d}^{-1}$ ; independent estimates of  $F_{NO_3^-}$ , based on the time-series dynamics of  $NO_3^-$  concentration profiles, suggested a minimum value of 241  $\mu\text{mol N m}^{-2} \text{ d}^{-1}$  and an upper limit of  $438 \pm 200$   $\mu\text{mol N m}^{-2} \text{ d}^{-1}$  (Johnson et al. 2010), a finding consistent with our results.

The range of  $\delta^{15}N$  values we have constrained for the upward  $NO_3^-$  flux (5–6‰) is consistent with measurements of  $\delta^{15}NO_3^-$  made in subeuphotic zone waters ( $\sim 200$ – $250$  m; Casciotti et al. 2008) that have ventilation times ranging between  $\sim 1$  yr and  $\sim 4$  yr (Bullister et al. 2006). Selection of shorter ventilation times ( $< 1$  yr), associated with waters with lighter  $\delta^{15}NO_3^-$  signatures, would not be expected to balance annual to multi-annual export fluxes. It seems likely that the very low  $\delta^{15}NO_3^-$  measurements at shallower depths previously reported in this region represent a transient situation; however, multiannual time-series measurements of the depth distribution of  $\delta^{15}NO_3^-$  would be necessary to test this hypothesis.

Assuming a C:N ratio of exported organic matter of 8:1 (Hannides et al. 2009), the range of  $F_{PN}$  modeled from our  $N_2$  fixation rate and  $\delta^{15}N\text{-PN}$  measurements (502–919  $\mu\text{mol N m}^{-2} \text{ d}^{-1}$ ) would be equivalent to an average downward organic carbon flux of 1.5 to 2.7  $\text{mol C m}^{-2} \text{ yr}^{-1}$ , an estimate consistent with various independent determinations of net community production (NCP) in this region (e.g., Keeling et al. 2004; Riser and Johnson 2008; Quay et al. 2010). Such results provide additional confidence in our constraint of the  $\delta^{15}N$  end-members selected for the two-source model.

Our use of the two-end-member isotope model and measured  $N_2$  fixation rates yielded estimates of  $F_{PN}$  that were greater than the  $F_{PN}$  values measured with sediment trap collections (Table 3). There are several potential reasons for this apparent mismatch. Undercollection of organic matter export based on sediment trap collection of sinking particles (including missed contributions from DON), alternate sources of fixed N to the upper ocean (e.g., atmospheric deposition or advection), and vertical and temporal variability in the  $\delta^{15}N$  signature of  $NO_3^-$  supplied to the euphotic zone all introduce uncertainties to the isotopic mass balance model. Although the flux of N to the upper ocean via atmospheric

deposition appears relatively small (Kim et al. 2014), the  $\delta^{15}\text{N}$  signature of N deposition often appears low ( $-4.5\text{‰}$  to  $-0.6\text{‰}$ ; Hastings et al. 2003; Knapp et al. 2008). As such, deposition of low  $\delta^{15}\text{N}$  to the upper ocean would result in overestimation of the contribution by  $\text{N}_2$  fixation based on the two end-member model. However, N supplied to the ocean via wet or dry deposition can derive from both natural (i.e., marine aerosols) and anthropogenic (i.e., fossil fuel combustion byproducts and fertilizers) sources. The  $\delta^{15}\text{N}$  signature of fertilizer  $\text{NO}_3^-$  ranges between  $-2\text{‰}$  and  $5\text{‰}$  (Heaton 1986), while fossil fuel combustion byproducts appear heavier, with  $\delta^{15}\text{N}$  signatures reported between  $6\text{‰}$  and  $13\text{‰}$  (Heaton 1990; Altieri et al. 2016). Hence, atmospheric transport and delivery of N from these sources has the potential to alter the isotopic composition of both the dissolved nutrient and particulate matter pools. If fossil fuel combustion byproducts are an increasingly important source of bioavailable N to the upper ocean at Station ALOHA as suggested by the recent study of Kim et al. (2014), such supply would increase the  $\delta^{15}\text{N}$  signature of sinking PN, leading to underestimation of the contribution of  $\text{N}_2$  fixation derived through use of the two end-member model, and therefore overestimating  $F_{\text{PN}}$ . Plankton assimilation of DON would further complicate the use of the two end-member model; measurements of the  $\delta^{15}\text{N}$  signature of high molecular weight DON in the upper ocean of the Pacific indicates a isotopic signature similar to that of deep ocean nitrate ( $5.4\text{‰} \pm 0.8\text{‰}$ ; Meador et al. 2007).

If our derived estimates of N export are correct, such results highlight potential undercollection of organic matter export by the sediment traps utilized for this study. The underlying assumption for the derived estimate of  $F_{\text{PN}}$  is that the  $\delta^{15}\text{N}$  signature of PN collected by sediment traps is representative of the export flux over annual to decadal time scales; while the total PN flux may be undercollected, we assume the traps are not biased with respect to the  $\delta^{15}\text{N}$  signature of the particles collected. Based on the time-integrated, average PN flux measured between 2006 and 2013 ( $272 \mu\text{mol N m}^{-2} \text{d}^{-1}$ ) and assuming a total N flux out of the upper 150 m between 505 and  $919 \mu\text{mol N m}^{-2} \text{d}^{-1}$  (Table 3), these results indicate that the sediment traps effectively collected between 30% and 54% of the organic N export during the present study (Table 3). Previous studies have described biases associated with the particle interceptor traps used for collecting sinking particles (Buesseler 1991; Michaels et al. 1994; Benitez-Nelson et al. 2001). Moreover, N export mediated by active zooplankton migration and excretion of  $\text{NH}_3$  at depth has been suggested to account for  $105 \pm 65 \mu\text{mol N m}^{-2} \text{d}^{-1}$ , and this flux would presumably not be accounted for in our trap-derived flux measurements (Hannides et al. 2009). In addition, sediment traps would not account for downward export of DON.

In conclusion, this study provides critical information on methodological challenges associated with direct oceanic  $\text{N}_2$  fixation rate measurements and reveals that  $\text{N}_2$  fixation is a

time-varying component of the ocean N cycle in the NPSG, and that variability in this process can be a major control on the magnitude of organic matter export in this ecosystem. Our results provide additional support highlighting that sediment trap-based estimates of NCP may be biased low while  $^{15}\text{N}$  tracer-based estimates appear to be consistent with previous reports of NCP (Emerson et al. 1997; Riser and Johnson 2008; Quay et al. 2010) and  $\text{NO}_3^-$  based new production (Johnson et al. 2010) in this region. Resolving whether sediment traps undercollect specific particle classes with differing  $\delta^{15}\text{N}$  remains an important and open question that needs to be resolved to fully interpret the  $\delta^{15}\text{N}$ -PN data record from Station ALOHA. Similarly, quantifying the importance of DON fluxes and zooplankton-mediated N transport, as possible pathways for fixed N export remains central to our ability to refine the upper ocean nitrogen budget in this ecosystem.

## References

- Abell, J., S. Emerson, and P. Renaud. 2000. Distributions of TOP, TON and TOC in the North Pacific Subtropical Gyre: Implications for nutrient supply in the surface ocean and remineralization in the upper thermocline. *J. Mar. Res.* **58**: 203–222. doi:[10.1357/002224000321511142](https://doi.org/10.1357/002224000321511142)
- Altieri, K. E., S. E. Fawcett, A. J. Peters, D. M. Sigman, and M. G. Hastings. 2016. Marine biogenic source of atmospheric organic nitrogen in the subtropical North Atlantic. *Proc. Natl. Acad. Sci. USA* **113**: 925–930. doi:[10.1073/pnas.1516847113](https://doi.org/10.1073/pnas.1516847113)
- Bauersachs, T., S. Schouten, J. Compaoré, U. Wollenzien, L. J. Stal, and J. S. S. Damsté. 2009. Nitrogen isotopic fractionation associated with growth on dinitrogen gas and nitrate by cyanobacteria. *Limnol. Oceanogr.* **54**: 1403–1411. doi:[10.4319/lo.2009.54.4.1403](https://doi.org/10.4319/lo.2009.54.4.1403)
- Beman, J. M., B. N. Popp, and S. E. Alford. 2012. Quantification of ammonia oxidation rates and ammonia-oxidizing archaea and bacteria at high resolution in the Gulf of California and eastern tropical North Pacific Ocean. *Limnol. Oceanogr.* **57**: 711–726. doi:[10.4319/lo.2012.57.3.0711](https://doi.org/10.4319/lo.2012.57.3.0711)
- Benitez-Nelson, C., K. O. Buesseler, D. M. Karl, and J. Andrews. 2001. A time-series study of particulate matter export in the North Pacific Subtropical Gyre based on  $^{234}\text{Th}$ :  $^{238}\text{U}$  disequilibrium. *Deep-Sea Res. I* **48**: 2595–2611. doi:[10.1016/S0967-0637\(01\)00032-2](https://doi.org/10.1016/S0967-0637(01)00032-2)
- Buesseler, K. O. 1991. Do upper-ocean sediment traps provide an accurate record of particle flux? *Nature* **353**: 420–423. doi:[10.1038/353420a0](https://doi.org/10.1038/353420a0)
- Bullister, J. L., D. P. Wisegarver, and R. E. Sonnerup. 2006. Sulfur hexafluoride as a transient tracer in the North Pacific Ocean. *Geophys. Res. Lett.* **33**: L18603. doi:[10.1029/2006GL026514](https://doi.org/10.1029/2006GL026514)
- Capone, D. G. 1993. Determination of nitrogenase activity in aquatic samples using the acetylene reduction

- procedure, p. 621–631. In P. Kemp, B. Sherr, E. Sherr, and J. Cole [eds.], *Handbook of methods in aquatic microbial ecology*. CRC Press.
- Capone, D. G., and J. P. Montoya. 2001. Nitrogen fixation and denitrification, p. 505–515. In J. Paul [ed.], *Methods in marine microbiology*, V. 30. Academic Press.
- Capone, D. G., and othres. 2005. Nitrogen fixation by *Trichodesmium* spp.: An important source of new nitrogen to the tropical and subtropical North Atlantic Ocean. *Glob. Biogeochem. Cycles* **19**: GB2024. doi:10.1029/2004GB002331
- Carpenter, E. J., H. R. Harvey, B. Fry, and D. G. Capone. 1997. Biogeochemical tracers of the marine cyanobacterium *Trichodesmium*. *Deep-Sea Res. I* **44**: 27–38. doi:10.1016/S0967-0637(96)00091-X
- Casciotti, K. L., T. W. Trull, D. M. Glover, and D. Davies. 2008. Constraints on nitrogen cycling at the subtropical North Pacific Station ALOHA from isotopic measurements of nitrate and particulate nitrogen. *Deep-Sea Res. II* **55**: 1661–1672. doi:10.1016/j.dsr2.2008.04.017
- Checkley, D. M., and C. A. Miller. 1989. Nitrogen isotope fractionation by oceanic zooplankton. *Deep-Sea Res. I* **36**: 1449–1456. doi:10.1016/0198-0149(89)90050-2
- Church, M. J., and D. Böttjer. 2013. Diversity, ecology, and biogeochemical influence of N<sub>2</sub>-fixing microorganisms in the sea, p. 608–625. In S.A. Levin [ed.], *Encyclopedia of biodiversity*, 2nd ed. Academic Press.
- Church, M. J., H. W. Ducklow, and D. M. Karl. 2002. Multi-year increases in dissolved organic matter inventories at Station ALOHA in the North Pacific Subtropical Gyre. *Limnol. Oceanogr.* **47**: 1–10. doi:10.4319/lo.2002.47.1.0001
- Church, M. J., C. Mahaffey, R. M. Letelier, R. Lukas, J. P. Zehr, and D. M. Karl. 2009. Physical forcing of nitrogen fixation and diazotroph community structure in the North Pacific Subtropical Gyre. *Glob. Biogeochem. Cycles* **23**: GB2020. doi:10.1029/2008GB003418
- Cline, J. D., and I. R. Kaplan. 1975. Isotopic fractionation of dissolved nitrate during denitrification in the eastern tropical North Pacific Ocean. *Mar. Chem.* **3**: 271–299. doi:10.1016/0304-4203(75)90009-2
- Dabundo, R., M. F. Lehmann, L. Treibergs, C. R. Tobias, M. A. Altabet, P. H. Moisander, and J. Granger. 2014. The contamination of commercial <sup>15</sup>N<sub>2</sub> gas stocks with <sup>15</sup>N-labeled nitrate and ammonium and consequences for nitrogen fixation measurements. *PLoS One* **9**: e110335. doi:10.1371/journal.pone.0110335
- Davis, C. S., and D. J. McGillicuddy. 2006. Transatlantic abundance of the N<sub>2</sub>-fixing colonial cyanobacterium *Trichodesmium*. *Science* **312**: 1517–1520. doi:10.1126/science.1123570
- Dore, J. E., and D. M. Karl. 1996. Nitrite distributions and dynamics at Station ALOHA. *Deep-Sea Res. II* **43**: 385–402. doi:10.1016/0967-0645(95)00105-0
- Dore, J. E., B. N. Popp, D. M. Karl, and F. J. Sansone. 1998. A large source of atmospheric nitrous oxide from subtropical North Pacific surface waters. *Nature* **396**: 63–66. doi:10.1038/23921
- Dore, J. E., J. R. Brum, L. M. Tupas, and D. M. Karl. 2002. Seasonal and interannual variability in sources of nitrogen supporting export in the oligotrophic subtropical North Pacific Ocean. *Limnol. Oceanogr.* **47**: 1595–1607. doi:10.4319/lo.2002.47.6.1595
- Dore, J. E., R. M. Letelier, M. J. Church, R. Lukas, and D. M. Karl. 2008. Summer phytoplankton blooms in the oligotrophic North Pacific Subtropical Gyre: Historical perspectives and recent observations. *Prog. Oceanogr.* **76**: 2–38. doi:10.1016/j.pocean.2007.10.002
- Duce, R. A., and others. 2008. Impacts of atmospheric anthropogenic nitrogen on the open ocean. *Science* **320**: 893–897. doi:10.1126/science.1150369
- Dugdale, R. C., and J. J. Goering. 1967. Uptake of new and regenerated forms of nitrogen in primary productivity. *Limnol. Oceanogr.* **12**: 196–206. doi:10.4319/lo.1967.12.2.0196
- Emerson, S. 2014. Annual net community production and biological carbon export in the ocean. *Glob. Biogeochem. Cycles* **28**: 1–12. doi:10.1002/2013GB004680
- Emerson, S., P. Quay, D. Karl, C. Winn, L. Tupas, and M. Landry. 1997. Experimental determinations of the organic carbon flux from open-ocean surface waters. *Nature* **389**: 951–954. doi:10.1038/40111
- Eppley, R. W., and B. J. Peterson. 1979. Particulate organic matter flux and planktonic new production in the deep ocean. *Nature* **282**: 677–680. doi:10.1038/282677a0
- Fong, A. A., D. M. Karl, R. Lukas, R. M. Letelier, J. P. Zehr, and M. J. Church. 2008. Nitrogen fixation in an anticyclonic eddy in the oligotrophic North Pacific Ocean. *ISME J.* **2**: 663–676. doi:10.1038/ismej.2008.22
- Galloway, J. N., and others. 2004. Nitrogen cycles: Past, present and future. *Biogeochemistry* **70**: 153–226. doi:10.1007/s10533-004-0370-0
- Garside, C., 1982. A chemiluminescent technique for the determination of nanomolar concentrations of nitrate and nitrite in seawater. *Mar. Chem.* **11**: 159–167. doi:10.1016/0304-4203(82)90039-1
- Großkopf, T., and others. 2012. Doubling of marine dinitrogen-fixation rates based on direct measurements. *Nature* **488**: 361–364. doi:10.1038/nature11338
- Guidi, L., and others. 2012. Does eddy-eddy interaction control surface phytoplankton distribution and carbon export in the North Pacific Subtropical Gyre. *J. Geophys. Res.- Biogeosci.* **117**: 02024. doi:10.1029/2012JG001984
- Hannides, C. C. S., M. R. Landry, C. R. Benitez-Nelson, R. M. Styles, J. P. Montoya, and D. M. Karl. 2009. Export stoichiometry and migrant-mediated flux of phosphorus in the

- North Pacific Subtropical Gyre. *Deep-Sea Res. I* **56**: 73–88. doi:[10.1016/j.dsr.2008.08.003](https://doi.org/10.1016/j.dsr.2008.08.003)
- Hastings, M. G., D. M. Sigman, and F. Lipschultz. 2003. Isotopic evidence for source changes of nitrate in rain at Bermuda. *J. Geophys. Res.* **108**. doi:[10.1029/2003JD003789](https://doi.org/10.1029/2003JD003789)
- Hebel, D. V., and D. M. Karl. 2001. Seasonal, interannual and decadal variations in particulate matter concentrations and composition in the subtropical North Pacific Ocean. *Deep-Sea Res. II* **48**: 1669–1696. doi:[10.1016/S0967-0645\(00\)00155-7](https://doi.org/10.1016/S0967-0645(00)00155-7)
- Heaton, T. H. E. 1986. Isotopic studies of nitrogen pollution in the hydrosphere and atmosphere: A review. *Atmos. Environ.* **21**: 843–852. doi:[10.1016/10168-9622\(80\)90059-x](https://doi.org/10.1016/10168-9622(80)90059-x)
- Heaton, T. H. E., 1990.  $^{15}\text{N}/^{14}\text{N}$  ratios of  $\text{NO}_x$  from vehicle engines and coal-fired power stations. *Tellus Ser. B* **42**: 304–307. doi:[10.1034/j.1600-0889.1990.00007.x](https://doi.org/10.1034/j.1600-0889.1990.00007.x)
- Jickells, T. D., and others. 2003. Isotopic evidence for a marine ammonia source. *Geophys. Res. Lett.* **30**: doi:[10.1029/2002GL016728](https://doi.org/10.1029/2002GL016728), 2003
- Johnson, K. S., S. C. Riser, and D. M. Karl. 2010. Nitrate supply from deep to near-surface waters of the North Pacific Subtropical Gyre. *Nature* **465**: 1062–1065. doi:[10.1038/nature09170](https://doi.org/10.1038/nature09170)
- Kana, T. M., C. Darkangelo, M. D. Hunt, J. B. Oldham, G. E. Bennett, and J. C. Cornwell. 1994. Membrane inlet mass spectrometer for rapid high-precision determination of  $\text{N}_2$ ,  $\text{O}_2$ , and Ar in environmental water samples. *Anal. Chem.* **66**: 4166–4170. doi:[10.1021/ac00095a009](https://doi.org/10.1021/ac00095a009)
- Karl, D. M., and G. Tien. 1992. MAGIC: A sensitive and precise method for measuring dissolved phosphorus in aquatic environments. *Limnol. Oceanogr.* **37**: 105–116. doi:[10.4319/lo.1992.37.1.0105](https://doi.org/10.4319/lo.1992.37.1.0105)
- Karl, D., R. M. Letelier, L. Tupas, J. E. Dore, J. Christian, and D. Hebel. 1997. The role of nitrogen fixation in biogeochemical cycling in the subtropical North Pacific Ocean. *Nature* **388**: 533–538. doi:[10.1038/41474](https://doi.org/10.1038/41474)
- Karl, D. M., and others. 2001. Ecological nitrogen-to-phosphorus stoichiometry at Station ALOHA. *Deep-Sea Res. II* **48**: 1529–1566. doi:[10.1016/S0967-0645\(00\)00152-1](https://doi.org/10.1016/S0967-0645(00)00152-1)
- Karl, D. M., R. R. Bidigare, M. J. Church, J. E. Dore, R. M. Letelier, C. Mahaffey, and J. Zehr. 2008. The nitrogen cycle in the North Pacific trades biome: An evolving paradigm, p. 705–769. *In* D. G. Capone, D. A. Bronk, M. R. Mulholland, and E. J. Carpenter [eds.], *Nitrogen in the marine environment*. Academic Press.
- Karl, D. M., M. J. Church, J. E. Dore, R. M. Letelier, and C. Mahaffey. 2012. Predictable and efficient carbon sequestration in the North Pacific Ocean supported by symbiotic nitrogen fixation. *Proc. Natl. Acad. Sci. USA* **112**: 1842–1849. doi:[10.1073/pnas.1120312109](https://doi.org/10.1073/pnas.1120312109)
- Keeling, C. D., H. Brix, and N. Gruber. 2004. Seasonal and long-term dynamics of the upper ocean carbon cycle at Station ALOHA near Hawai'i. *Glob. Biogeochem. Cycles* **18**: GB4006. doi:[10.1029/2004GB002227](https://doi.org/10.1029/2004GB002227)
- Kim, I. N., K. Lee, N. Gruber, D. M. Karl, J. L. Bullister, S. Yang, and T. W. Kim. 2014. Increasing anthropogenic nitrogen in the North Pacific Ocean. *Science* **346**: 1102–1106. doi:[10.1126/science.1258396](https://doi.org/10.1126/science.1258396)
- Knapp, A. N., P. J. DiFiore, C. Deutsch, D. M. Sigman, and F. Lipschultz. 2008. Nitrate isotopic composition between Bermuda and Puerto Rico: Implications for  $\text{N}_2$  fixation in the Atlantic Ocean. *Glob. Biogeochem. Cycles* **22**: GB3014. doi:[10.1029/2007GB003107](https://doi.org/10.1029/2007GB003107)
- Knapp, A. N., K. L. Casciotti, W. M. Berelson, M. G. Prokopenko, and D. G. Capone. 2016. Low rates of nitrogen fixation in eastern tropical South Pacific surface waters. *Proc. Natl. Acad. Sci. USA* **113**: 4398–4403. doi:[10.1073/pnas.1515641113](https://doi.org/10.1073/pnas.1515641113)
- Knauer, G. A., J. H. Martin, and K. W. Bruland. 1979. Fluxes of particulate carbon, nitrogen, and phosphorus in the upper water column of the northeast Pacific. *Deep-Sea Res. I* **26**: 97–108. doi:[10.1016/0198-0149\(79\)90089-X](https://doi.org/10.1016/0198-0149(79)90089-X)
- Letelier, R. M., D. M. Karl, M. R. Abbott, and R. R. Bidigare. 2004. Light driven seasonal patterns of chlorophyll and nitrate in the lower euphotic zone of North Pacific Subtropical Gyre. *Limnol. Oceanogr.* **49**: 508–519. doi:[10.4319/lo.2004.49.2.0508](https://doi.org/10.4319/lo.2004.49.2.0508)
- Mahaffey, C., C. R. Benitez-Nelson, R. R. Bidigare, Y. Rii, and D. M. Karl. 2008. Nitrogen dynamics within a wind-driven eddy. *Deep-Sea Res. II* **55**: 1398–1411. doi:[10.1016/j.dsr2.2008.02.004](https://doi.org/10.1016/j.dsr2.2008.02.004)
- Meador, T. B., L. I. Aluwihare, and C. Mahaffey. 2007. Isotopic heterogeneity and cycling of organic nitrogen in the oligotrophic ocean. *Limnol. Oceanogr.* **52**: 934–947. doi:[10.4319/lo.2007.52.3.0934](https://doi.org/10.4319/lo.2007.52.3.0934)
- Michaels, A. F., N. R. Bates, K. O. Buesseler, C. A. Carlson, and A. H. Knap. 1994. Carbon-cycle imbalances in the Sargasso Sea. *Nature* **372**: 537–540. doi:[10.1038/372537a0](https://doi.org/10.1038/372537a0)
- Mohr, W., T. Großkopf, D. W. R. Wallace, and J. LaRoche. 2010. Methodological underestimation of oceanic nitrogen fixation rates. *PLoS One* **59**: e12583. doi:[10.1371/journal.pone.0012583](https://doi.org/10.1371/journal.pone.0012583)
- Montoya, J. P., M. Voss, P. Kahler, and D. G. Capone. 1996. A simple, high-precision, high-sensitivity tracer assay for  $\text{N}_2$  fixation. *Appl. Environ. Microbiol.* **62**: 986–993.
- Montoya, J. P., C. M. Holl, J. P. Zehr, A. Hansen, T. Villareal, and D. G. Capone. 2004. High rates of  $\text{N}_2$  fixation by unicellular diazotrophs in the oligotrophic Pacific Ocean. *Nature* **430**: 1027–1031. doi:[10.1038/nature02824](https://doi.org/10.1038/nature02824)
- Moore, C. M., and others. 2013. Processes and patterns of oceanic nutrient limitation. *Nat. Geosci.* **6**: 701–710. doi:[10.1038/ngeo1765](https://doi.org/10.1038/ngeo1765)
- Ostrom, N. E., M. E. Russ, B. Popp, T. M. Rust, and D. M. Karl. 2000. Mechanisms of nitrous oxide production in the subtropical North Pacific based on determinations of the isotopic abundances of nitrous oxide and di-oxygen.



- Chemosphere-Glob. Chang. Sci. **2**: 281–290. doi:[10.1016/S1465-9972\(00\)00031-3](https://doi.org/10.1016/S1465-9972(00)00031-3)
- Paulot, F., and others. 2015. Global oceanic emission of ammonia: Constraints from sea-water and atmospheric observations. *Glob. Biogeochem. Cycles* **29**: 1165–1178. doi:[10.1002/2015GB005106](https://doi.org/10.1002/2015GB005106)
- Quay, P. D., C. Peacock, K. Björkman, and D. M. Karl. 2010. Measuring primary production rates in the ocean: Enigmatic results between incubation and non-incubation methods at Station ALOHA. *Glob. Biogeochem. Cycles* **24**: GB3014. doi:[10.1029/2009GB003665](https://doi.org/10.1029/2009GB003665)
- Riser, S., and K. Johnson. 2008. Net production of oxygen in the subtropical ocean. *Nature* **451**: 323–325. doi:[10.1038/nature06441](https://doi.org/10.1038/nature06441)
- Robidart, J. C., and others. 2014. Ecogenomic sensor reveals controls on N<sub>2</sub>-fixing microorganisms in the North Pacific Ocean. *ISME J.* **8**: 1175–1185. doi:[10.1038/ismej.2013.244](https://doi.org/10.1038/ismej.2013.244)
- Santoro, A. E., C. Buchwald, M. R. McIlvin, and K. L. Casciotti. 2011. Isotopic composition of N<sub>2</sub>O produced by marine ammonia-oxidizing archaea. *Science* **333**: 1282–1285. doi:[10.1126/science.1208239](https://doi.org/10.1126/science.1208239)
- Saino, T., and A. Hattori. 1987. Geographical variation of the water column distribution of suspended particulate organic nitrogen and its <sup>15</sup>N natural abundance in the Pacific and its marginal seas. *Deep-Sea Res. I* **34**: 807–827. doi:[10.1016/0198-0149\(87\)90038-0](https://doi.org/10.1016/0198-0149(87)90038-0)
- Sigman, D. M., and others. 2009. The dual isotope of deep nitrate as a constraint on the cycle and budget of oceanic fixed nitrogen. *Deep-Sea Res. I* **56**: 1419–1439. doi:[10.1016/j.dsr.2009.04.007](https://doi.org/10.1016/j.dsr.2009.04.007)
- Sohm, J. A., E. A. Webb, and D. G. Capone. 2011. Emerging patterns of marine nitrogen fixation. *Nat. Rev. Microbiol.* **9**: 499–508. doi:[10.1038/nrmicro2594](https://doi.org/10.1038/nrmicro2594)
- Thompson, A., and J. P. Zehr. 2013. Cellular interactions: Lessons learned from the nitrogen-fixing cyanobacteria. *J. Phycol.* **49**: 1024–1035. doi:[10.1111/jpy.12117](https://doi.org/10.1111/jpy.12117)
- Wada, E., and A. Hattori. 1976. Natural abundance of <sup>15</sup>N in particulate organic matter in the North Pacific Ocean. *Geochim. Cosmochim. Acta.* **40**: 249–251. doi:[10.1016/0016-7037\(76\)90183-6](https://doi.org/10.1016/0016-7037(76)90183-6)
- Wilson, S. T., D. Böttjer, M. J. Church, and D. M. Karl. 2012. Comparative assessment of nitrogen fixation methodologies conducted in the oligotrophic North Pacific Ocean. *Appl. Environ. Microbiol.* **78**: 6516–6523. doi:[10.1128/AEM.01146-12](https://doi.org/10.1128/AEM.01146-12)
- Zehr, J. P., and R. M. Kudela. 2011. Nitrogen cycle of the open ocean: From genes to ecosystems. *Ann. Rev. Mar. Sci.* **3**: 197–225. doi:[10.1146/annurev-marine-120709-142819](https://doi.org/10.1146/annurev-marine-120709-142819)

### Acknowledgments

The authors extend special thanks to the Hawai'i Ocean Time-series scientists and staff for their help and support in facilitating this work. Additionally, we thank S. Ferrón for assistance with running the membrane inlet mass spectrometer and to D. Viviani for support with statistical analyses. We also acknowledge the captains and crews of the research vessels *Kilo Moana* and *Kaimikai-O-Kanaloa*. Nitrate isotopic data from Casciotti et al. (2008) were obtained from the Biological and Chemical Oceanography Data Management Office (<http://www.bco-dmo.org/dataset/2971/data>). This research was supported by grants from the National Science Foundation (OCE09-26766; OCE08-50827; and DBI04-24599). Additional support was derived from the Simons Collaboration on Ocean Processes and Ecology (SCOPE) and the Gordon and Betty Moore Foundation (project #3794).

### Conflict of Interest

None declared.

Submitted 16 September 2015

Revised 21 April 2016

Accepted 11 July 2016

Associate editor: Anya Waite